# INFLUENCE OF CARBON NANOPARTICLES/EPOXY MATRIX INTERACTION ON MECHANICAL, ELECTRICAL AND TRANSPORT PROPERTIES OF STRUCTURAL ADVANCED MATERIALS*

Liberata Guadagno[1,*], Carlo Naddeo[1,*], Marialuigia Raimondo[1],

Giuseppina Barra[1], Luigi Vertuccio[1], Salvatore Russo[2], Khalid Lafdi[3],

Vincenzo Tucci[4], Giovanni Spinelli[4], Patrizia Lamberti[4]

*[1]Department of Industrial Engineering, University of Salerno,*

*Via Giovanni Paolo II, 132, 84084, Fisciano (SA), Italy.*

*[2]Leonardo-Finmeccanica SpA, Engineering and Industrialization / New Airframe*

*Technologies, Viale dell'Aeronautica, Pomigliano D'Arco (NA), 80038, Italy.*

*[3]University of Dayton, 300 College Park Dayton Ohio 45440.*

*[4]Department of Information and Electrical Engineering and Applied Mathematics,*

*University of Salerno, Via Giovanni Paolo II, 132, 84084, Fisciano (SA), Italy.*

***Corresponding author***

***Liberata Guadagno - e-mail: lguadagno@unisa.it***

***phone +39 089964114***

***Carlo Naddeo - e-mail: cnaddeo@unisa.it***

*phone +39 089964019*

## ABSTRACT

The focus of this study is to design new nano-modified epoxy formulations using carbon nanofillers, such as carbon nanotubes (CNTs), carbon nanofibers (CNFs) and graphene-based nanoparticles (CpEG), that reduce the moisture content and provide additional functional performance. The chemical structure of epoxy mixture, using a non-stoichiometric amount of hardener, exhibits unique properties in regard to the water sorption for which the equilibrium concentration of water ($C_{eq}$) is reduced up to a maximum of 30%. This result, which is very relevant for several industrial applications (aeronautical, shipbuilding industries, wind turbine blades, etc.), is due to a strong reduction of the polar groups and/or sites responsible to bond water molecules. All nanofillers are responsible of a second phase at lower glass transition temperature (Tg). Compared with other carbon nanofillers, functionalized graphene-based nanoparticles exhibit the best performance in the multifunctionality. The lowest moisture content, the high performance in the mechanical properties, the low electrical percolation thereshold (EPT) have been all ascribed to particular arrangements of the functionalized graphene sheets embedded in the polymeric matrix. Exfoliation degree and edge carboxilated groups are responsible of self-assembled architectures which entrap part of the resin fraction hindering the interaction of water molecules with the polar sites of the resin, also favoring the EPT paths and the attractive/covalent interactions with the matrix.

**Keywords:** Water transport properties, Thermosetting resin, Carbon based nanocomposites, MWCNTs, CNFs, Graphene-based nanoparticles.

## 1. Introduction

A number of several interrelated factors have to be taken into account in the design of functional nanocomposites for structural applications. A proper selection of matrix and nanofiller, together with the fascinating prospect of transferring the appealing properties of nanostructures to the final product, can allow to meet specific and heavy requirements able to breach the wall of the current limitations in significant areas of industrial applications. The recent ability of material scientists in the control of matter behavior at nanoscale level can be exploited to design a new generation of emerging materials able to simultaneously satisfy several structural and functional requirements. For instance, in the field of primary aeronautical structures, through a tailored transfer of nanoparticle properties to the structural resins, new potential perspectives are foreseen. Low-weight green aircrafts at low fuel consumption make feasible substantial decreases in the cost and environmental impact, simultaneously enhancing material performance. The benefits of resistant low-weight composites, compared to the usual metal-alloys, have led to the recent trend of increased use of the former with respect to the more traditional metallic components. The coming of the new age of the carbon-fibre reinforced composites has been primarily driven by the urgent need to reduce the weight of load-bearing structures and hence cost and environmental impact. It has been found that 1 kg of saved fuel due to a weight reduction of an aircraft primary structure results in a reduction of 3.15 Kg of $CO_2$ emission into the atmosphere [1]. Furthermore, the high resistance to fatigue and corrosion, the good mechanical performance of carbon fiber reinforced composites make them particularly suitable for light and resistant structures able to withstand the aerodynamic loads and other mechanical stress [2].

At the same time, several drawbacks of these materials prohibit their use to the extent where instead their full potential could be exploited. In this regard, strong limitations are due to the impossibility of current aeronautical materials to satisfy special needs able to meet the high standards and fulfil the

requirements in this field [3]. In service condition, in fact, aircraft materials can be subjected to atmospheric hazards (lightning, icing, heavy precipitation, hail, etc.) and/or adverse environmental conditions (strong humidity, wide temperature variations, etc.) [4].

Functional nanocomposites can be designed to possess attributes beyond the basic strength and stiffness that typically drive the science and engineering of the material for structural systems. For instance, currently rotor blades for wind energy turbines and aeronautical components (fuselage, wings, etc.) are usually made of glass-fibre or carbon-fiber reinforced resins which are insulating materials. To head off the remarkable risk of a puncture of structural parts, during a lightning event, or in general to optimize optical, electromagnetic and mechanical properties of the formulation, higher electrical and thermal conductivities are required. These properties must be imparted without additional weight and preserving the corrosion resistance typical of a composite material (e.g without high concentration of metallic particles or metallic skins on the panels).

Very low amounts of electrical conductive nanoparticles embedded in epoxy resin, or introduced between-lamina interfaces, can help for example to address limitations related to the electrical and thermal insulating properties which negatively impact on the design of anti-lightning properties, anti-icing systems and thermal dissipation phenomena [5-9].

Furthermore, water transport properties, such as diffusion and sorption of water in aeronautical resins must be driven towards the smallest possible values. It is well known, in fact, that water vapor absorption decreases the performance of aircraft materials for the adverse effects on the physico-mechanical properties, corrosion and weight [5]. Data concerning the effect of water absorption on the mechanical performance of structural resins highlight a significant lowering of the glass transition temperature (Tg) and consequently the degradation of high-temperature properties [5]. Petherick et al. found that the lowering in Tg is determined by disruption of strong hydrogen bonds in the cured network, and their replacement with weaker water-related hydrogen bonds [10]. In the area of load-bearing materials for application in aeronautics, marine industry etc. many papers deal with the

problem of the moisture content of the TetraGlycidyl-MethyleneDiAniline (TGMDA) solidified with 4,4'-diaminodiphenyl sulfone (DDS) for its peculiar properties which are suitable for higher operating temperatures maintaining at the same time high performance in mechanical properties. Despite these top-flight characteristics, in many cases the more common bifunctional epoxy precursor DGEBA is used because the water content absorbed by epoxy resins based on TGMDA is higher than DGEBA and other epoxy precursors applied as structural resins. In fact, TGMDA/DDS systems are reported to absorb as much as 6.5 wt% water; Liu et al. reported for this system a value of 7.76% (at 23 °C) [11] and Li et al. the value of 6.48% (at 35 °C) [12]. A higher water content results in a dramatic drop in Tg [13-14]. In this paper, a nanofilled epoxy resin, able to overcome criticalities related to insulating properties and based on TGMDA/DDS system characterized by a low moisture content, is described. The use of a reactive diluent diluent, 1,4-butandiol diglycidyl ether (BDE), inside the unfilled and nanofilled epoxy precursor based on TGMDA has proven to be of benefit for decreasing the viscosity of the epoxy matrix [15-16]. This decrease is particularly advantageous for thermosetting resins filled with nanoparticles which tend to dramatically increase the viscosity of the resin [6,17].

Furthermore, the appropriate choice of the nature and amount of hardening agent can reduce the moisture absorbed in the epoxy matrix giving low values in the equilibrium concentration of water ($C_{eq}$) also after conditioning the samples at 120 °C under vacuum for 24 h. This last experimental procedure has proven to be very effective to remove also the bonded water in the molecular structure. Experimental results highlight that the chemical structure of the formulated epoxy mixture (using a non-stoichiometric amount of hardener) manifests peculiar properties with respect to the water sorption due to a strong reduction in the number of polar groups and sites able to bond water molecules also in the case of nanofilled formulations. MWCNTs, CNFs and CpEG nanoparticles have been embedded into the epoxy formulation and the effect of nanofillers on the water transport properties and mechanical and electrical performance has been investigated. Combined advantages originated by suitable carbon based nanoparticles and phase composition of the resin can open

potential perspectives of the formulated nanocomposites in the field of specific multifunctional applications.

The interrelated nature of aspects concerning the moisture transport in unfilled and nanofilled amine-cured epoxy resins is studied and discussed with the aim to simultaneously obtain an enhancement in relevant physical properties which generally act in complementary way. The multifunctionality is a real challenge for the scientist materials, in fact, in the nanotechnology field, frequently the improvement in some properties results in the decrease of others. As an instance, functionalized conductive nanoparticles are able to increase compatibility with the matrix and in many case also mechanical properties but in the meanwhile the functionalization acts in opposite way on the electrical properties. This paper highlights that specific functionalizations of graphene-based nanoparticles act in a synergic way for improving mechanical, electrical and water transport properties of structural resins. The results have been studied and compared with other common nanofillers such as CNTs and CNFs.

## 2. Experimental part

### *2.1. Materials*

The epoxy matrix was prepared by mixing the tetraglycidylmethylenedianiline (TGMDA) (epoxy equivalent weight 117–133 g/eq), with the epoxy monomer 1-4 butanedioldiglycidyl ether (BDE). The 4,4′-diaminodiphenyl sulfone (DDS) was used as hardener agent. The epoxy mixture was prepared by mixing TGMDA with the reactive monomer BDE monomer at a concentration of 80%:20% (by wt) epoxide to diluent. The curing agent was added at stoichiometric and non-stoichiometric amount with respect to the epoxy rings (TGMDA and BDE). The sample hardened with a stoichiometric amount of DDS without reactive diluent is named TGMDA+DDS, whereas the sample with reactive diluent is named TGMDA/BDE+DDS. For the samples where the hardener agent was added at non-

stoichiometric ratios of amine/epoxy, DDS at 44.4 phr was used. This resin was named TGMDA/BDE+DDS(NS).

The reactive monomer BDE is very effective in improving the curing degree of nanofilled epoxy mixtures [6]. It increases the mobility of reactive groups resulting in a higher cure degree than the epoxy precursor alone [6]. This effect is particularly advantageous for resins filled with nanoparticles where higher temperature treatments are needed, compared to the unfilled resin, to reach the same cure degree.

In this paper, different carbon nanostructured particles, CNTs, CNFs, CpEG were dispersed in the epoxy mixture with the aim obtain an enhancement in relevant physical properties. It is well known from the literature that different nanostructured forms of carbon can be employed to impart functional properties to the hosting polymeric matrix or can be dispersed in the polymer as mechanical reinforcements. Currently, carbon nanofillers are obtained using several methods resulting in different morphological features, structures and functionalization nature. A thorough knowledge of the correlations between structural/morphological characterization and nanofiller/hosting matrix properties necessarily requires a laborious and accurate analysis. Data here shown are discussed also in light of previous publications [4,17-18] in which a deep analysis of the nanofiller properties and the role of the structural parameters and functionalization nature on the properties of the resulting nanocomposites have been investigated; so the reader is referred to the previous articles for the detailed characterization.

The MWCNTs (3100 Grade) were from Nanocyl S.A. They are characterized by an outer diameter ranging from 10 to 30 nm and a length from hundreds of nanometers to some micrometer. Walls number varies from 4 to 20 and the specific surface area is around 250-300 $m^2/g$ (Brunauer–Emmett–Teller method). The carbon purity is higher than 95% and the metal oxide impurity is lower than 5% (thermogravimetric analysis).

CNFs powders were from Applied Sciences Inc. (Pyrograf III family). The CNFs used in this study were heat-treated at 2500 °C (acronym CNFs) to obtain the best combination in their electrical and mechanical properties [18].

The sample of graphene-based nanoparticles consists of carboxylated partially exfoliated graphite (CpEG). It has been prepared with the aim to simultaneously enhance mechanical, electrical and water transport properties of structural resins. This sample was prepared using an exfoliation procedure from natural graphite through a traditional acid intercalation by using a mixture containing nitric and sulphuric acid followed by rapid expansion occurring after a sudden treatment at high temperature (900 °C) [19]. This particular procedure allows to obtain a partially exfoliated graphite with edge-carboxylated layers (CpEG) having a two dimensional (2D) predominant shape. In this paper, a sample characterized by a degree of exfoliated phase of 60% was used.

### *2.2. Preparation of nanocomposites*

Epoxy blend and DDS were mixed at 120 °C and the nanofillers were added and incorporated into the matrix via ultrasonication for 20 min. An ultrasonic device, Hielscher model UP200S (200 W, 24 kHz) was used. The epoxy mixture TGMDA/BDE+DDS was loaded with nanofillers at two different concentrations (0.5% and 1% by wt). These nanofiller concentrations were chosen because the curves of dc volume conductivity vs. nanofiller concentration highlighted that the nanofilled samples were beyond the electrical percolation threshold (EPT) [18-19]. All the unfilled and filled epoxy mixtures were cured at 125 °C for 1 h and 200 °C for 3 h. In this paper, composites with CNTs, CNFs and CpEG are named X (type of nanofiller) (NS), where X represents the nanofiller percentage and (NS) is the acronym for the non-stoichiometric formulations. As example, 0.5%CpEG(NS) is the epoxy mixture TGMDA/BDE+DDS(NS) filled with CpEG nanofiller at 0.5% concentration w/w%. Similary, 0.5% CpEG is the epoxy mixture TGMDA/BDE+DDS filled with CpEG nanofiller at 0.5% concentration w/w%.

*2.3. Characterization*

*2.3.1. Transport Properties*

The fully cured epoxy resins have been cut into samples with dimensions of 40×20×0.50 $mm^3$ immediately after the curing cycle. The thickness of the water absorption test samples was made small, deliberately, compared to its width and length, such as edge effects could be ignored and simple one-dimensional diffusion model analysis can be applied without incurring significant error.

After conditioning samples at 120 °C under vacuum for 24 h to ensure complete dryness, the specimens were placed into distilled water chambers maintained at constant temperature of 25 °C. This methodology has been selected after different mechanical tests which have proven that the drastic treatment at 120 °C under vacuum for 24 h is able to remove all the water in the resin (including bound water). This also causes the disappearance of the peak related to the presence of bound water in the dynamic mechanical spectrum.

The specimens were weighed periodically using a digital balance with 0.01 mg resolution to determine the percent weight change, and, thus, water uptake. The water gain percentage, $C_t$ %, was determined from the eq. 1:

$$C_t = \frac{W_t - W_d}{W_t} * 100 \quad \text{(eq. 1)}$$

In eq. 1, $W_t$ is the weight of the water-sorbed epoxy specimen at t time and $W_d$ is the initial weight of the dry specimen. The equilibrium concentration of water $C_{eq}$ was calculated considering the maximum amount of absorbed water (plateau condition in Fig. 1).

The specimens were periodically removed, dried and immediately weighed, and then returned to the water bath. The step of drying is performed to ensure the removal of excessive surface (superficial) water, specimens were gently wiped dry using clean, lint-free tissue paper.

The described absorption procedure yielded a series of water gain versus time curves (see Figs 1-2 of the next section).

### *2.3.2. SEM Analysis*

Micrographs of the epoxy nanocomposites based on the carbon nanofillers CNTs, CNFs and CpEG were obtained using SEM (mod. LEO 1525, Carl Zeiss SMT AG, Oberkochen, Germany). All the samples were placed on a carbon tab previously stuck to an aluminium stub (Agar Scientific, Stansted, UK) and were covered with a 250 Å-thick gold film using a sputter coater (Agar mod. 108 A). Nanofilled sample sections were cut from solid samples by a sledge microtome. These slices were etched before the observation by SEM. The etching reagent was prepared according to a previous reported procedure [5].

### *2.3.3. Dynamic mechanical analysis*

Dynamic mechanical properties of the samples were performed with a dynamic mechanical thermo-analyzer (Tritec 2000 DMA -Triton Technology). Solid samples with dimensions 2x10x 35 $mm^3$ were tested by applying a variable flexural deformation in three points bending mode. The displacement amplitude was set to 0.03 mm, whereas the measurements were performed at the frequency of 1 Hz. The range of temperature was from -90 °C to 315 °C at the scanning rate of 3 °C/min.

### *2.3.4. FT/IR analysis*

FTIR spectra were obtained at a resolution of 2.0 $cm^{-1}$ with a FTIR (BRUKER Vertex70) spectrometer equipped with deuterated triglycine sulfate (DTGS) detector and a KBr beam splitter, using KBr pellets. The frequency scale was internally calibrated to 0.01 $cm^{-1}$ using a He−Ne laser. 32 scans were signal averaged to reduce the noise.

*2.3.5. Electrical Properties*

The electrical characterization of the nanocomposites focused on the DC volume conductivity was performed on disk shaped specimens of about 2 mm of thickness and 50 mm of diameter. In order to reduce possible effects due to surface roughness and to ensure an ohmic contact with the measuring electrodes, the samples were coated by using a silver paint with a thickness of about 50 μm and characterized by a surface resistivity of 0.001 Ω·cm. The measurement system, remotely controlled by the software LABVIEW®, is composed by a suitable shielded cell with temperature control, a multimeter Keithley 6517A with function of voltage generator (max ±1000V) and voltmeter (max ± 200 V) and an ammeter HP34401A (min current 0.1μA) for samples above the Electrical Percolation Threshold (EPT), whereas for those below EPT a multimeter Keithley 6517A with function of voltage generator (max ±1000V) and pico-ammeter (min current 0.1 fA) is used.

## 3. Results and discussion

*3.1. Characterization of epoxy matrix and carbon/epoxy composites: water transport properties*

Figure 1 illustrates the curves reporting the data of water concentration vs. time for the unfilled epoxy mixtures for a water activity (a=1) at the temperature of 25 °C.

As described in the experimental section, the samples have been conditioned at 120 °C under vacuum for 24 h to ensure complete dryness and then the specimens were placed into distilled water chambers maintained at constant temperature of 25 °C.

Formulations hardened using non-stoichiometric and stoichiometric amount of curing agent (DDS) have been analysed. As described in the experimental section, in part of the formulations, DDS was added at a non-stoichiometric amount (80% by weight with respect to the stoichiometric amount) (acronym sample: TGMDA/BDE+DDS(NS)).

The sorption at equilibrium of liquid water ($C_{eq}$) decreases from 6.81% (TGMDA+DDS) to 5.76% for the sample TGMDA/BDE+DDS solidified in stoichiometric concentration of hardener and to 4.83% for the sample TGMDA/BDE+DDS(NS) solidified in non-stoichiometric condition. The resin reduces the value in $C_{eq}$ from a minimum of 15% at a maximum of 30%. This percentage is very relevant for application of epoxy resins in aeronautics or other structural applications because absorbed moisture increases the weight of the structures and determines a reduction of the matrix-dominated mechanical properties.

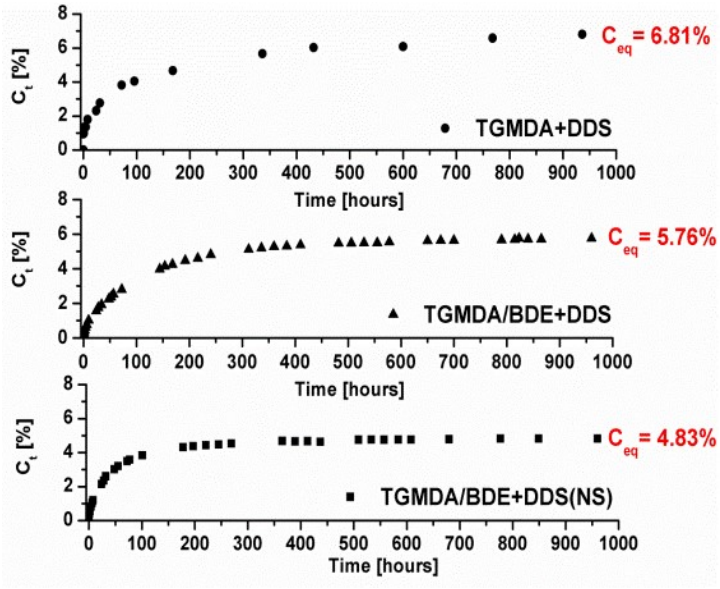


**Figure 1**. The concentration at time ($C_t$) as a function of the time (hours) of the epoxy resin (without BDE), and the epoxy mixture containing the diluent at stoichiometric and non-stoichiometric ratios of amine/epoxy.

The epoxy mixture TGMDA/BDE+DDS(NS) hardened with a non-stoichiometric ratio of hardener, for which the most significant reduction in $C_{eq}$ was observed, has been selected to prepare the nanocomposites filled with the chosen nanoparticles. Figure 2 illustrates the curves reporting the data of water concentration vs. time for the epoxy mixtures filled with CNTs, CNFs and CpEG at two different concentrations. The experimental conditions are the same used to collect the data of Figure 1. Figure 3 shows the sorption values at equilibrium (Ceq) of liquid water of the different tested

nanofilled resins. Data shown in Figures 2-3 highlight that, also at high water activity (a=1), the nanofilled samples are characterized by values of $C_{eq}$ only slightly higher than the unfilled matrix. Hence, these data prove that advantages in the water transport properties can be combined with the better mechanical and electrical performance of the nanofilled formulations.

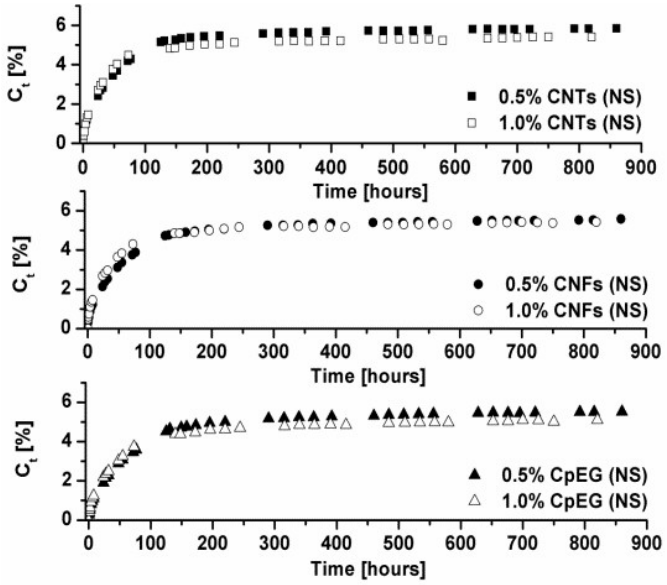


**Figure 2.** The concentration at time ($C_t$) as a function of the time (hours) of epoxy mixtures filled with CNTs, CNFs and CpEG at 0.5 wt% and 1.0 wt%.

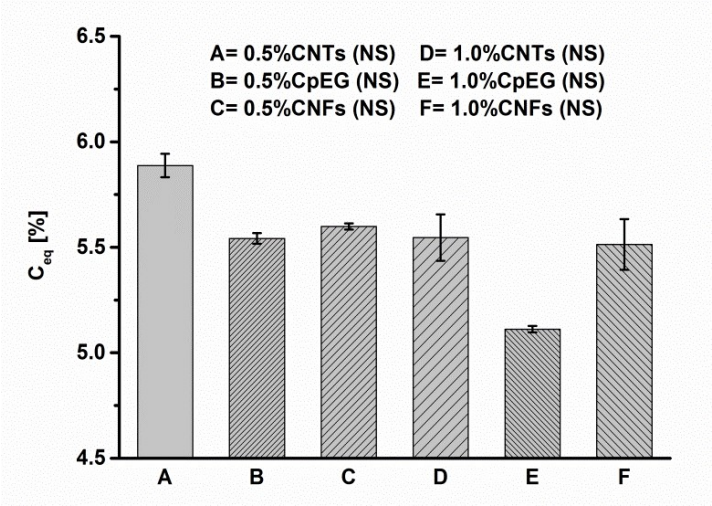


**Figure 3.** The sorption values at equilibrium ($C_{eq}$) of liquid water of the various tested nanofilled resins.

It is also evident that for the same nanofiller, an increase in the nanofiller concentrations causes a decrease in the sorption values. The best results are obtained using CpEG as nanofiller. It is worth noting that the structural and morphological analysis highlighted that this sample is composed by graphene layers and very thin graphitic blocks; it represent the best combination to optimize mechanical and electrical properties of nanofilled samples also with respect to graphene single layers [19]. This result evidences that the presence of graphene sheets and thin graphite blocks together with the nature of the epoxy matrix certainly create a synergistic effect that makes this sample especially suitable in the field of structural resins such as aeronautical, nautical and wind turbine materials. This beneficial effect can be exploited in addition to other very promising properties of graphene based materials [19-29]. In Figure 4, we observe a Fickian behavior that is a linear dependence of the reduced sorption on square root of time, a curvature for $C_t/C_{eq}$> 0.7 and a constant value at equilibrium.

This Fickian behavior gives the possibility to derive the diffusion parameter, D, by the first linear part of the curve, by the eq. (2).

$$\frac{C_t}{C_{eq}} = \frac{4}{d}\left(\frac{Dt}{\pi}\right)^{\frac{1}{2}} \quad \text{(eq. 2)}$$

where $C_{eq}$ is the equilibrium concentration of water, $C_t$ the concentration at time t, d (cm) is the thickness of the sample, and D ($cm^2/s$) the mean diffusion coefficient. The diffusion parameter, D ($cm^2s^{-1}$), of the analysed samples, is shown in Table 1. The value of D is between $1.31x10^{-9}$ and $1.83x10^{-9}$ $cm^2/s$. It is evident that the diffusion of water molecules into the samples with different nanofillers follows the same curve. These results highlight that the small percentage of nanofiller (max 1%) has no effect on the diffusion coefficient. If we compare the results related to the sample TGMDA/BDE+DDS with data reported for the TGMDA+DDS system (without BDE), we can note that a lower value of absorbed water is obtained for the epoxy mixture TGMDA/BDE+DDS(NS) and also for the nanofilled epoxy resins.

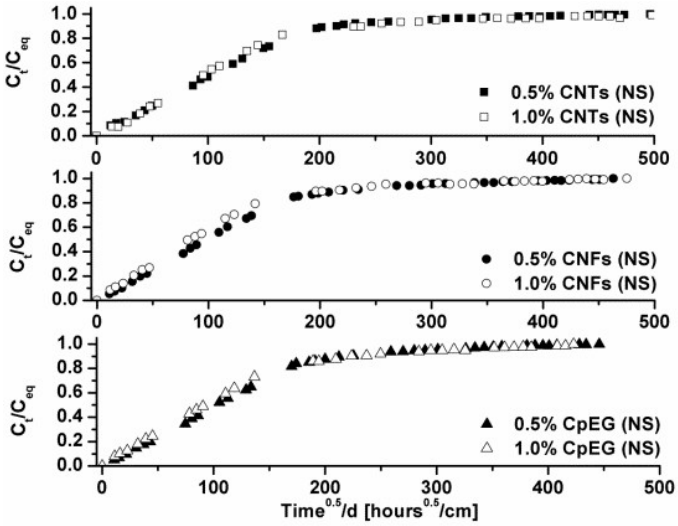


**Figure 4.** $C_t/C_{eq}$ against the square root of time of the resin with 0.5% and 1.0% of CNTs, CNFs and CpEG.

**Table 1**
The diffusion parameter, D ($cm^2s^{-1}$), of the analysed samples.

| Samples | D ($cm^2/s$) |
|---|---|
| TGMDA/BDE+DDS (NS) | 1.39E-09 ± 4.94E-10 |
| 0.5%CNTs (NS) | 1.25E-09 ±3.40E-11 |
| 0.5%CpEG (NS) | 1.52E-09 ±2.60E-10 |
| 0.5%CNFs (NS) | 1.31E-09 ±1.08E-10 |
| 1.0%CNTs (NS) | 1.44E-09 ±5.45E-11 |
| 1.0%CpEG (NS) | 1.36E-09 ±1.71E-10 |
| 1.0%CNFs (NS | 1.83E-09 ±1.51E-10 |

This value is almost comparable with the value obtained for DGEBA cured with DDS in stoichiometric amount (4.03%) or cured with a tertiary amine which leads to polyetherification by nucleophilic ring opening of oxirane ring originating a network with significant differences [30]. compared with those obtained with primary amines as in the case of the present paper.

### *3.2. Morphological Investigation*

#### *3.2.1. Morphological investigation of the carbon based epoxy nanocomposites*

The nanofiller dispersion in the polymeric matrix was analyzed by SEM investigation on etched samples. Figure 5 shows SEM images of the fracture surface of the three epoxy-based composites filled with 0.5 wt% loading of nanofillers (CNTs, CNFs and CpEG, respectively). The etching procedure consumes part of the surface layers of the epoxy matrix. A very relevant result is observed for the sample filled with CpEG. In fact, the same etching procedure is more efficient for the resins loaded with CNTs and CNFs, where we can observe whole lengths of the CNTs and CNFs segments to emerge from the consumed resin. In both cases, the nanofillers seems uniformly dispersed in the polymeric matrix. The observation of the image in Figure 5 also highlights that only a few layers of graphene appear clearly visible in the surface, emerging from the epoxy resin. This is a clear evidence that strong interconnections between CpEG particles and epoxy matrix remain after the etching attack. Graphene-based nanoparticles seem to enhance the CpEG/epoxy matrix interaction hindering the resin consumption in regions located around the nanofiller. This effect may be responsible of the more efficient load transfer and consequently of the strong mechanical reinforcement in the elastic modulus as described in the following section on dynamic mechanical properties of the nanocomposites.

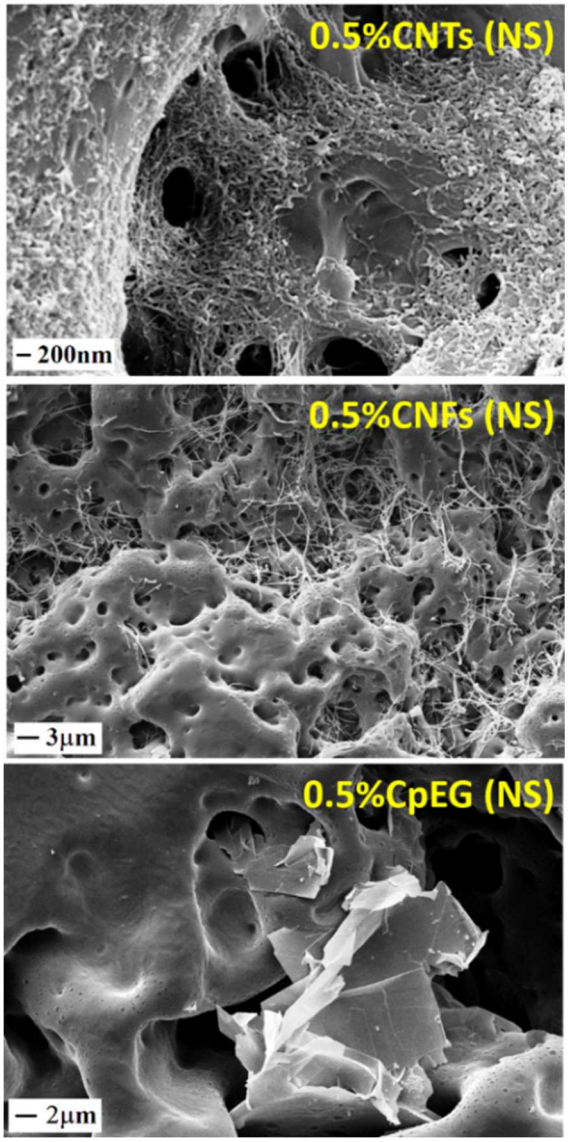


**Figure 5.** SEM images of the fracture surface of the three different epoxy nanocomposites with 0.5 wt% loading of nanofillers.

### *3.3.Dynamic Mechanical Analysis (DMA)*

In order to fully understand the influence of carbon nanofillers (CNTs, CNFs, CpEG) on the unfilled and nanofilled epoxy-amine resins hardened in stoichiometric and non-stoichiometric condition, dynamic mechanical analysis was performed. The storage modulus, E' (MPa), and the loss factor,

tanδ, of the unfilled epoxy formulation, and the composites with a concentration of 0.5% by weight of nanoparticles are shown in Figures 6-7.

All the samples show very high values of the storage modulus in the normal operational temperature range of structural materials; E' is higher than 2000 MPa in the very wide temperature range of -100 ÷ 100 °C. The profile of the curves in Figure 6 shows a slow and progressive decrease of E' up to 50 °C, followed by an almost constant value in the range between 50÷200 °C before the principal drop, due to the glass transition temperature Tg which is evident between 200÷300 °C. The presence of the Tg in this range is also confirmed by the mechanical spectrum of the samples shown in Figure 7. In particular, the highest peak, which is associated with the samples glass transition, or α transition, in the mechanical spectra is centred at 262 °C for the unfilled sample, 261 °C for the sample filled with CNTs, 260 °C for the sample with CNFs and 266 °C for the sample with CpEG. It is worth noting that for this type of nanofilled sample an increase in the activation energy E2 related to secondary amine-epoxy reaction was also found [31].

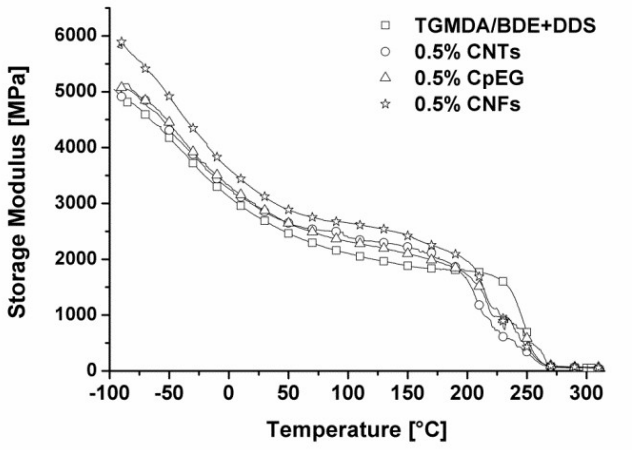


**Figure 6.** Storage modulus of the unfilled epoxy formulation (TGMDA/BDE+DDS) and epoxy formulations at loading rate of 0.5% by weight of CNTs, CpEG and CNFs.

This increase was ascribed to self-assembly structure generated by the edge-carboxylated layers of graphite nanoparticles inside the epoxy matrix in such a way to form architectures constituted of rigid nano-cages where the final curing reactions must be active under condition of more reduced mobility with respect to the conditions experimented by other mono-dimensional nanofillers [31].

To better understand the influence of the nanofiller on the α transition, and also to avoid confusing effects with the effect of hardener amount, a non-stoichiometric amount of hardener has been also employed to solidify the unfilled epoxy formulation before to draw conclusions on the nanocharged samples. Figure 8a shows the loss factor (tanδ) of the unfilled epoxy formulations TGMDA/BDE+DDS(NS) hardened with the chosen non-stoichiometric amount of DDS. The loss factor of the sample solidified in stoichiometric ratio of hardener is also shown for comparison. The intensity of the main transition, α transition, is affect by the stoichiometry and therefore by the curing degree of the resin, furthermore samples hardened with non-stoichiometric amount exhibit two distinct peaks most likely due to fractions with different crosslinking density characterized by two different values of Tg (see Figure 8b). The more the peak at a lower Tg raises, the more the peak at a higher Tg decreases, suggesting that the two phases can coexist in the resin with different percentages depending on the stoichiometric amount of hardener. Furthermore, in the unfilled sample hardened in stoichiometric condition, the epoxide oxygen seems to be involved in a much more amount of crosslinking bonds, also limiting crankshaft rotation of the glycidyl crosslinking segments, on the contrary of what occurs in the sample cured in non-stoichiometric amount of DDS. In fact, it is evident in Figure 8a that the other two weak transitions, the β transition (between -100 and 30 °C) and the γ transition (between 30 and 120÷140 °C) are much more pronounced. It has been suggested that the β transition can be due to crankshaft rotations of the glycidyl crosslinking segments [32-33], it also represents stress relaxation which contributes the toughness of diamine-cured epoxy formulation.

Whereas, unreacted molecular segments and/or material inhomogeneities from region of different crosslink density could be responsible for the γ transition.

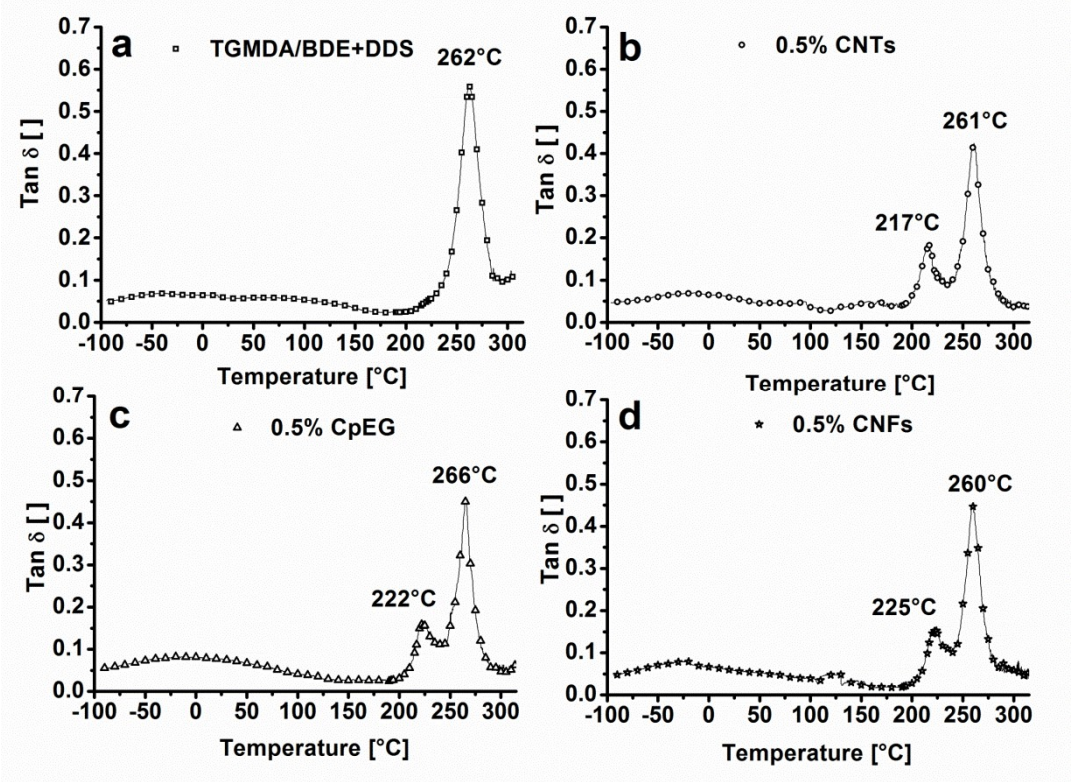


**Figure 7.** Loss factor (tanδ) of the unfilled epoxy formulation a) TGMDA/BDE+DDS and epoxy formulations at loading rate of 0.5% by weight of b) CNTs, c) CpEG and d) CNFs.

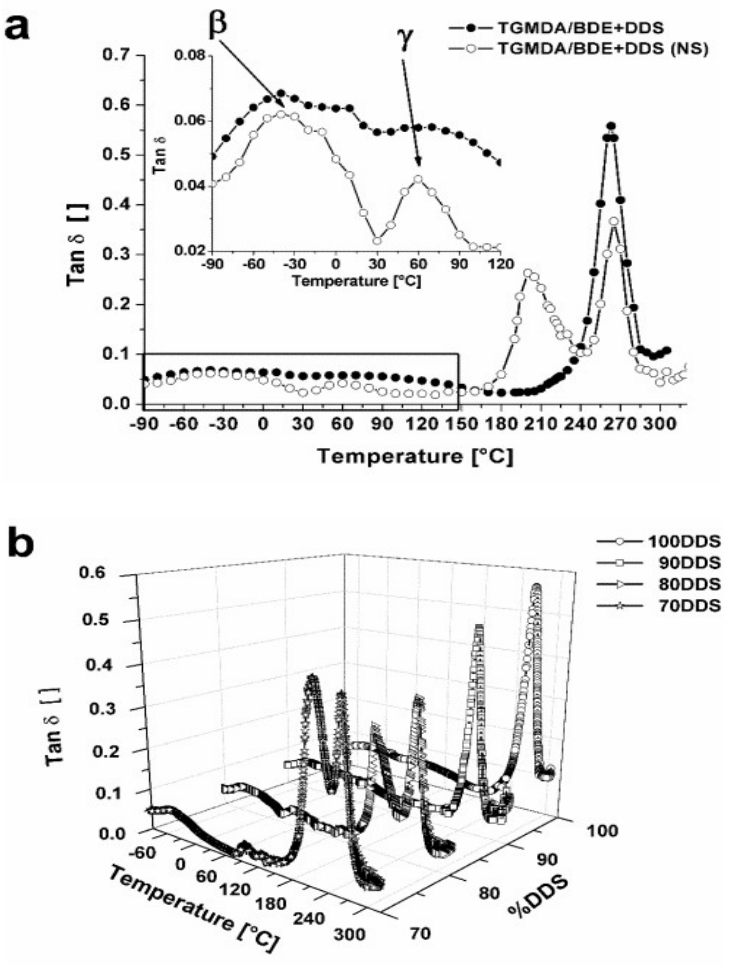


**Figure 8.** Loss factor (tanδ) of the unfilled epoxy formulation: a) stoichiometric system (TGMDA/BDE+DDS) and non-stoichiometric system (TGMDA/BDE+DDS(NS)); b) Loss factor (tanδ) of the unfilled epoxy formulations hardened with stoichiometric and different non-stoichiometric amounts of DDS.

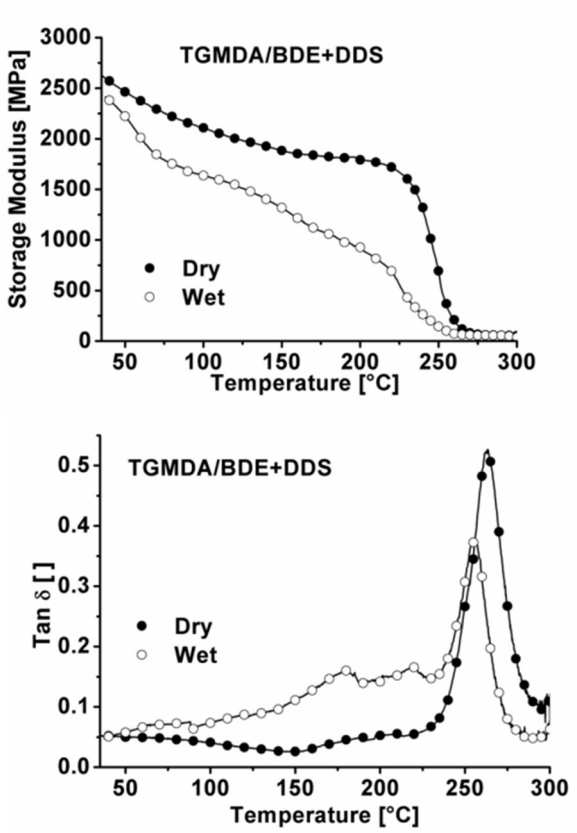


**Figure 9.** Loss factor (tanδ) and Storage Modulus of the dry and wet epoxy formulation hardened with a stoichiometric ratio of DDS (TGMDA/BDE+DDS).

It is worth noting that the entity of the observed transitions is also dependent on the moisture content (see Figure 9) where the Loss factor (tanδ) and the storage modulus of the wet sample (immersed in water for 1000 h before the DMA analysis) solidified in stoichiometric condition are shown together with the curves of the dry sample of Figure 8a. The moisture content shifts the main peak to lower temperatures (252 °C) and causes the appearance of other two transition centred at 220 °C and 180 °C respectively. These transitions are strictly related to plasticization effects caused by absorbed water. For this reason, as described in the experimental part, all the samples under investigations have been conditioned at 120 °C under vacuum for 24 h before the DMA analysis. This condition has proven to be very effective to eliminate also bonded water molecules. The described treatment allows to simplify

the understanding on the influence of the hardener ratio on the mechanical spectrum. This consideration has been also applied to the formulated nanocomposites.

It is worth noting that for many papers reported in literature, a such drastic treatment has not been performed; hence the understanding of the effect the nanofiller on the mechanical spectrum is complicated by overlapping effects. To study the effect of nanofiller on the dynamic mechanical properties of the epoxy formulations; all the nanocomposites were analysed in completely dry conditions. Considering that all the nanocharged samples solidified in stoichiometric conditions have been cured using the same curing cycle, it is evident that the nanofiller exerts on the resin the same influence of a non-stoichiometric amount of DDS. This behaviour is also confirmed by the data of Figure 10 which shows the reaction enthalpy and the curing degree for the unfilled and filled systems cured in stoichiometric conditions. The inclusion of the filler causes a decrease of the reaction enthalpy and the curing degree.

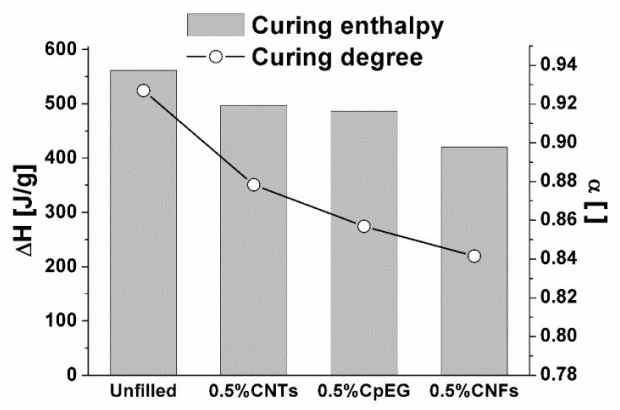


**Figure 10**. Reaction enthalpy and the curing degree of unfilled samples and filled samples (0.5% by weight of nanofiller).

These results are most likely due to an interruption of the cross-linking reactions during the curing cycle. It is well known that this interruption leads to a change in the glass transition temperature [34]. In our case, the introduction of the filler into a tetra-functional epoxy precursor, does not determine a significant change in the main glass transition temperature (see Figure 7), but the formation of a

fraction of the resin with a lower Tg. In fact, the transitions in the mechanical spectra at 217 °C (CNTs), 222 °C (CpEG) and 225 °C (CNFs) represent a phase with greater mobility of chain segments, most probably closely linked to the filler. All the analysed nanofillers are responsible for forming in the resin a second phase characterized by different crosslinking density with different values of Tg depending on the nanofiller nature. In this regard, it can be noticed that the value of the Tg at higher temperature is 260/261 °C, almost the same, for the samples filled with CNT and CNFs, whereas for the sample with CpEG this value is 266 °C. This increase could be due to the nature of the functionalized graphene-based nanoparticles. For this type of nanoparticles, it has been proven that, due to the high exfoliation degree and the role of edge-carboxylated graphite layers, the nanoparticles are able to give self-assembled structures embedded in the polymeric matrix [19]. Dynamic mechanical curves shown in Figure 11 evidence that graphene layers inside the matrix may serve as building blocks which may hinder the chain mobility resulting in a higher Tg (main transition). It is worth noting that this increase in Tg cannot be caused by a higher curing degree because as described before, the inclusion of all filler causes a lack of homogeneity in the cross-linking density with a lower curing degree (see Figure 10). The effect of the filler on many mechanical parameters of the nanocharged polymers is hard to understand in light of different data in literature. Carbon nanoparticles are widely used as a reinforcing agent in epoxy resins for improving their mechanical, thermal and electrical properties. It is well known that the addition of carbon nanoparticles into the resin matrix can dramatically change its hardness, tensile strength, elastic modulus and electrical conductivity [35]. Specifically, the effects of the nanofillers in polymer composites on the glass transition (Tg) and on the relaxation behaviour of the polymer matrix have been studied for different filled composites. However, the remarks on Tg variation are controversial as in some cases an increase in Tg with filler content is reported in the literature [36], yet the opposite result is possible as well. Furthermore, the variation of Tg as a function of filler content in epoxy nanocomposites shows an initial decrease up to a certain content value followed by an increase at higher filler loading. A

coherent picture among all data described in literature is almost impossible due to significant changes in the amount of components, in the nature of hardener, epoxy precursor and nanofiller, and most of all in the curing cycles and dispersion methods adopted by different authors. Furthermore, the entity of the nanofiller reinforcing effect was also found to be strongly dependent on the nature of the epoxy formulation [5,30]. Therefore, the actual effect of the filler on the Tg necessitates further clarification. In general, the amount, the dispersion and the surface characteristics of the nanoparticles were found to play an important role in the variation of Tg and the mechanical properties of the nanocomposites. In epoxy nanocomposites and generally in thermoset nanocomposites there is an additional difficulty with respect to the thermoplastic nano-composites. In particular, the curing conditions of the nanocomposites and related results are different from those of the pure epoxy probably due to the effect of the nanoparticles on the crosslinking mechanisms. In the present paper, the effect of the nanofiller on Tg and storage modulus has been analyzed by choosing the appropriate conditions/parameters to keep constant: matrix nature, ratio of epoxy precursor/ hardener, curing cycles and studied/controlled treatments to avoid the presence of free and bound water molecules in the matrix, which can also be responsible of changes in the mechanical parameters. The DMA curves of Figures 6-7 show that the introduction of the filler (in completely dry samples) increases the storage modulus of few hundred MPa, in the range from room temperature to 200 °C, for the CpEG and the CNTs system, around a thousand of MPa, in the range of temperature from -90 to 200 °C for the CNFs system for the same amount of nanoparticles. For all the filled systems a new glass transition is obtained at lower temperatures. The height and width of the peaks in tan delta spectra provide additional information about the relaxation behaviour of these samples. The height of the main peak at 262 °C for the neat resin has a value 0.60, while for the nanocomposites, it varies between 0.40 and 0.45. This implies that the nanocomposites exhibit more elastic behaviour than the neat resin. The change in the width of the peak at higher temperature suggests a narrow distribution of relaxation times for the resin filled with nanoparticles, presumably due to a phase segregation of the more cured

resin at high crosslinking density from the domains where nanoparticle/polymer interactions are relevant, and hence a different mobility is expected for this second phase at lower Tg. This indicates, at a first glance, the existence of at least two underlying mechanisms of alfa-relaxation. The first mechanism (higher Tg) is caused by the reaction of the crosslinking agent with the epoxy groups giving rise to the dominant alfa-relaxation, while the second one appears as a result of the fillers effect on the curing reaction. The formation of a few nm thick intermediate layer on the resin-filler interface, probably occurs before the full cure of the composite, thereby inducing the growth of the secondary peak at lower Tg. On the other hand, due to the impossibility to extend the tri-dimensional network in the space filled by the nanoparticles, a more mobile phase also composed of network segments polymerized by chain extension is expected in the zones around the nanofiller surfaces. Concerning the effect of the nanofiller on the resin hardened in non-stoichiometric conditions, a synergism between nanofiller effect and low DDS level is observed. Figure 11 shows the storage modulus (a, c and e) and the loss factor (tanδ) (b, d, f) of the unfilled epoxy formulation TGMDA/BDE+DDS(NS) and epoxy formulations at loading rate of 0.5% and 1% by weight of: CNTs (CNTs system), CNFs (CNFs system), and CpEG (CpEG system). In Figure 11, the non-stoichiometric systems are considered for two different percentages of nanoparticles to understand the effect of the filler concentration.

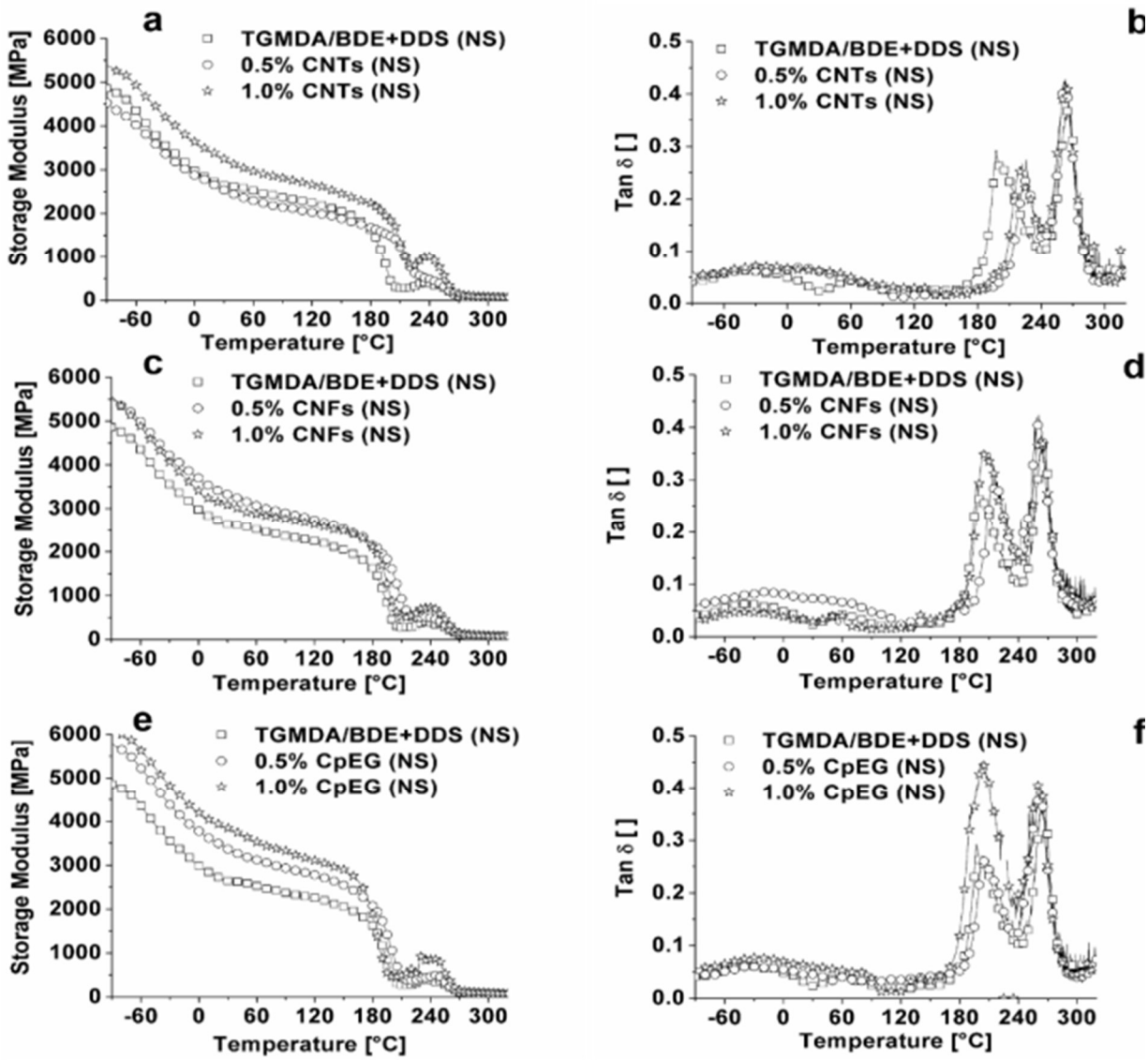


**Figure 11.** Storage modulus (a, c and e) and the loss factor (tanδ) (b, d, f) of the unfilled epoxy formulation TGMDA/BDE+DDS(NS) and epoxy formulations at loading rate of 0.5% and 1% by weight of: CNTs, CpEG and CNFs hardened in non-stoichiometric condition.

It can be observed that, compared with the sample in Figure 7, the height of the peak corresponding to the lower Tg is relevant, because the inclusion of nanofiller and the non-stoichiometric amount of hardener cause the same effects. Furthermore, wide and temperature of this peak is strongly dependent on the amount and nature of the filler. In the sample filled with 1% by weight of CpEG, the entity of

this peak is more relevant with respect to the peak at higher Tg (see Figure 11f), and correspondingly a strong reinforcement effect is observed in the storage modulus (see Figure 11e). The higher amount of nanofiller (1%) with respect to the amount of 0.5% also causes a noticeable broadening of the peak highlighting that many of the mechanical properties of the material (damping effect, toughness, flexibility etc..) are completely different from the unfilled sample. A reinforcing effect is observed for all the nanofillers (except for CNTs at lower concentration of filler), and the more reinforcing effect is observed for CpEG. It is worth noting that, in the resin filled with CpEG, the carboxylated groups on the edges of graphene/graphitic blocks strongly interact with the layer at lower Tg, also forming resin cured with different mechanisms due to the effect of carboxylated groups on the curing mechanisms of the resin surrounding the graphene/graphitic layers. Nanofiller functionalization can provide superb polymer–particle interactions which are very effective for improving the mechanical characteristics, but at same time may worsen electrical conductivity of the nanofilled polymer as it occurs for functionalized CNFs (without graphitization treatment at 2500 °C) [18]. In the nanocomposites filled with CpEG nanoparticles, we get a significant advancement on these two fronts simultaneously and on the transport properties of the nanocomposite. These simultaneous enhancements in the different properties are most likely due to the same effect already described in a previous paper [19]. In particular, self-assembly mechanisms determined by attractive interactions based on hydrogen bonding between edge-carboxylated graphitic blocks, were found. The presence of very thin graphitic block self-assembled along the samples is able to increase mechanical and electrical properties, but also able to further reduce the moisture content. Another important consideration concerns the interaction of CNTs with the epoxy matrix; even if the sample of CNT (3100 Grade) was known (from Nanocyl S.A.) as non-functionalized filler; the Raman and FT/IR spectra [5] do not correspond to carbon nanotube surfaces completely devoid of functional groups on the walls. This causes a non-negligible reinforcing effect (see storage modulus of the unfilled and filled samples in Figure 11a) most of all at concentration of filler higher than 0.5 by weight. Fortunately, many data already

described in literature can be used to understand the observed behaviors. In fact, although epoxy resins can be cured with different families of hardeners, most studies so far performed have been devoted to different aspects related to epoxy resins cured with amine curing agents. In cured epoxies, the three dimensional molecular structure determines the glass transition temperature and, as consequence, many physical properties of the material. In turn, the molecular network structure depends on the chosen pre-polymers, the curing agent nature, the stoichiometric ratio, the cure cycle and the advance of cross-linking reaction as well. Changes in network structure invariably cause modifications in chemical, physical and mechanical properties of the material. Therefore, while it is of the utmost importance to establish a set of correlations between the chemistry, the processing and the physical properties, this task results of a formidable difficulty and many parameters have to be fixed to investigate just one aspect of the problem. In particular, from the chemical point of view, it is well known that the cure reactions of epoxy resins are very complex because many reactive processes simultaneously occur; furthermore other events, such as gelation and vitrification phenomena, the autocatalytic effect in the early stages of curing, and the change from chemical control to diffusion control in the later stages of curing, can complicate the analysis. The cross-linking reactions between epoxy pre-polymers and amine hardeners generally involve the opening of the epoxy ring by reaction with amine hydrogen or with the formed hydroxyl (etherification reaction), as shown in Figure 12. This scheme consists in: 1) primary amine addition; 2) secondary amine addition; 3) etherification. The intensive cross-linking occurring in the region between the above transitions reduces molecular mobility, and the cure changes from a kinetic to a diffusion regime. The etherification reaction can occur between a hydroxyl group formed in the first stage, and an epoxy to form an ether link.

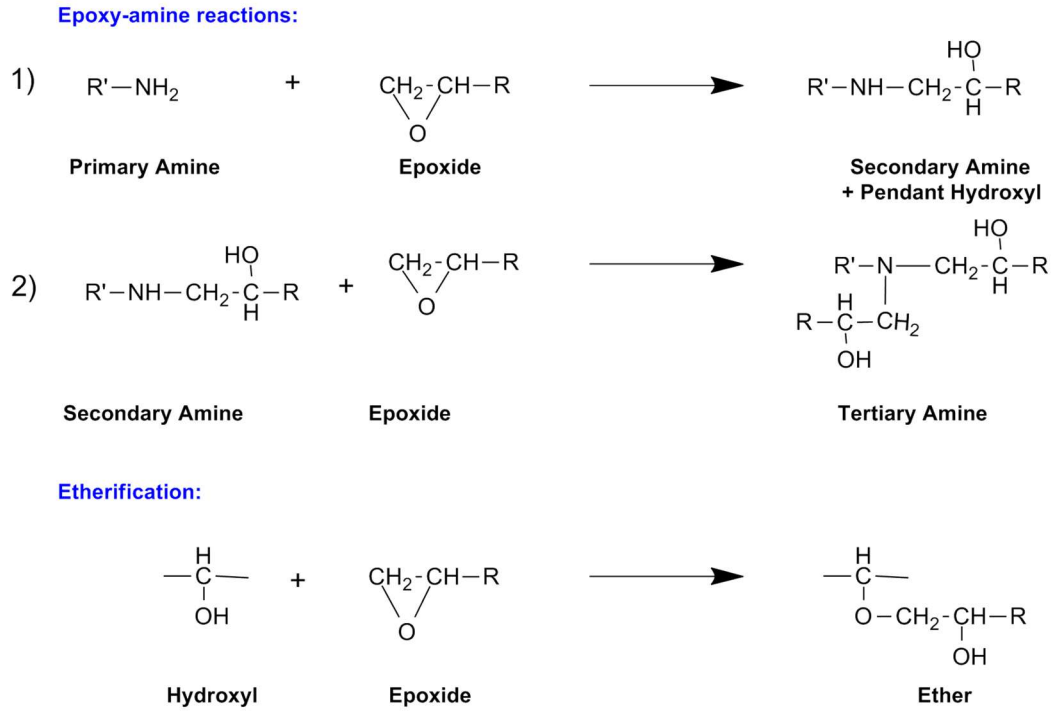


**Figure 12.** Scheme of cross-linking reactions between epoxy pre-polymers and amine hardeners.

This etherification reaction can also occur with the catalytic effect of a tertiary amine or other additives in the cure mixture, and in this case it is called homo-polymerization, not giving a network but a linear polymer. In this paper, to simplify the complexity of the different systems and better understand the effect of the different fillers, the competition between the possible paths of the cure reaction has been firstly studied by varying the stoichiometric ratio between epoxy and amine hardeners using the same epoxy formulation and curing cycle. Indeed, it has been recognized that a variation of the stoichiometric ratio of epoxy to curing agent can have a significant effect on the final mechanical properties of the cured resin, and therefore this is one of the most important aspect to be taken into account before considering the effect of the nanofillers. In conclusion, a very important result of this investigation is that the filler tends to create a phase with increased mobility of the

chains, segmental parts of the epoxy network around the filler which causes an increase in the more mobile phase (which is also caused by defect of hardener). In fact, the transition at lower temperature can represent chain segments partially cured or chain segments obtained by etherification reactions between functional groups of the filler and epoxy precursors. These kinds of reactions are also expected in unfilled samples cured with non-stoichiometric amount of hardener. In this case, the etherification reaction is expect to be more relevant with respect to the samples cured using a stoichiometric amount of hardener. Considering the effect of high epoxy/amine ratios compared to the stoichiometric system, both phenomena occur in the nanofilled formulations containing embedded CNTs and most of all CpEG. The etherification reactions between functional groups on the nanofiller surface and the epoxy resin determine a reinforcing effect of the nanofiller because the load is better transferred to the high strength nanofiller. This is reflected in the increase of the storage modulus, whereas the etherification reactions inside the epoxy resin, non-involving the nanofiller, determine a decrease in the storage modulus. Of course, these effects are balanced in nanofilled epoxy mixture cured in no-stoichiometric conditions.

### *3.4 FTIR Analysis*

Figure 13 shows the FT/IR spectra of the unfilled epoxy formulations hardened with non-stoichiometric amount of DDS in two different spectral ranges: a) range 3700-2700 $cm^{-1}$, b) range 1700-400 $cm^{-1}$. The reactions 1) and 2) of the scheme in Figure 12, namely primary amine addition and secondary amine addition are completed for all the samples, also for the sample hardened with a stoichiometric amount of DDS (TGMDA/BDE+DDS). In fact, no N-H signals are observed in all spectra shown in Figure 13a. In particular, primary amines for which two weak absorption bands (N-H stretching vibrations), one at 3471 $cm^{-1}$ and the other near 3373 $cm^{-1}$ are expected, are completely absent. The absence of these bands indicates that no “free” asymmetrical and symmetrical N-H

stretching modes are active in the samples. Also the band at 3240 $cm^{-1}$ which is the Fermi resonance band with overtone of the band at 1617 $cm^{-1}$ related to the N-H bend (scissoring) is absent. Secondary amines show a single weak band in the 3350-3310 $cm^{-1}$ region.

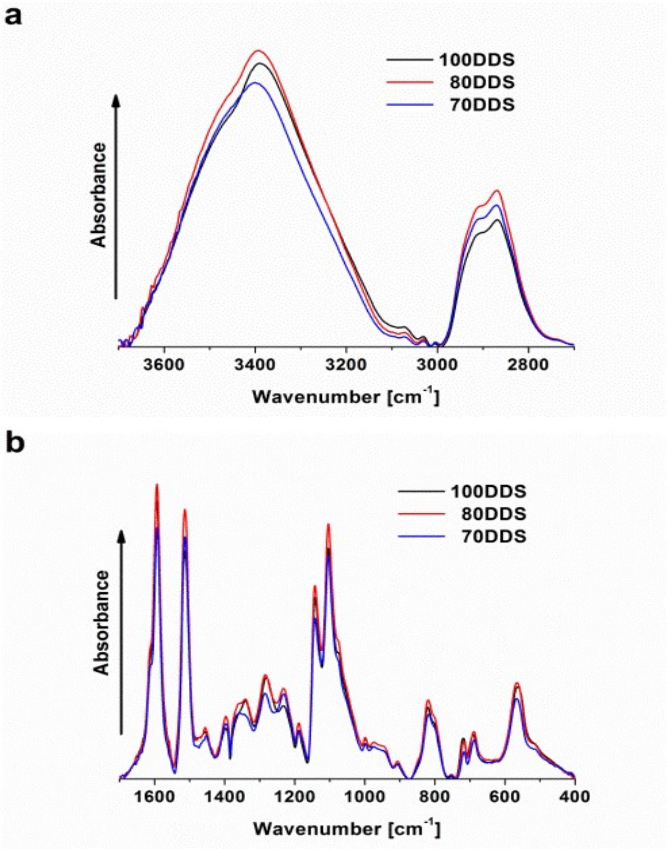


**Figure 13.** FT/IR spectra of the unfilled epoxy formulations hardened with non-stoichiometric amount of DDS in two different spectral ranges: a) range 3700-2700 $cm^{-1}$, b) range 1700-400 $cm^{-1}$.

The absence of this last signal also proves the completion of the secondary amine addition. In the region between 3000 and 3750 $cm^{-1}$, the spectra only show the O-H stretching vibration with a typical profile of stretching modes involved in intermolecular hydrogen bonding. Figure 14 shows an enlargement of the spectra in the region between 1150-1400 $cm^{-1}$ where the most significant changes of the spectra can be observed. In the range 1310-1360 $cm^{-1}$, the C-N stretch at 1341 $cm^{-1}$ of tertiary

aromatic amines are visible for all the samples. This signal is higher and well-defined in the sample solidified in stoichiometry condition. It overlaps with the asymmetric $SO_2$ stretching (DDS) between 1300-1350 $cm^{-1}$. This last signal is expected to be less intense for the sample 70DDS and 80DDS with respect to the sample solidified in stoichiometric condition of hardener (100 DDS). The signal of the O-H bending vibration centered at 1360 $cm^{-1}$ seems to be more relevant for the samples solidified in non-stoichiometric condition due to the decrease C-N stretch signal at 1341 $cm^{-1}$. A similar effect is observed for the peaks at 1232 $cm^{-1}$ due to C-O stretching vibration of secondary alcohols. They seem more intense for the samples 80DDS and 70DDS with respect to the sample TGMDA/BDE+DDS because the band at 1280 $cm^{-1}$ is less intense in the samples 80DDS and 70DDS. In light of these spectroscopic results and studies already available from the literature, we can explain the low moisture content of samples hardened in non-stoichiometric conditions.

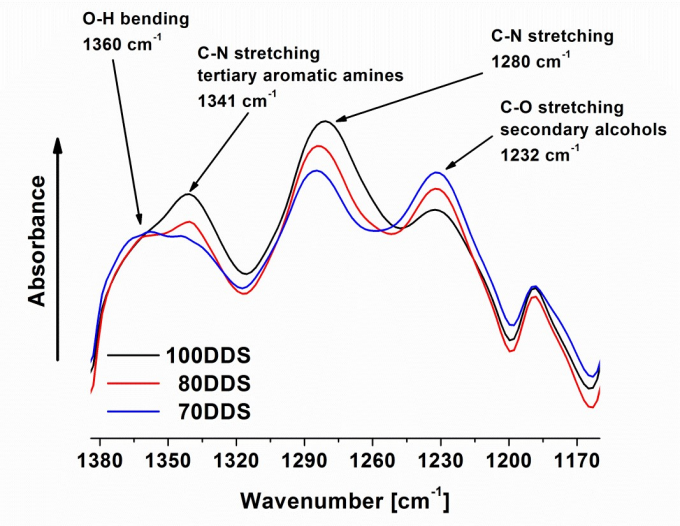


**Figure 14.** FT/IR spectra in the range 1150-1450 $cm^{-1}$ of the unfilled epoxy formulations hardened with stoichiometric and non-stoichiometric amount of DDS.

A careful study of the molecular mechanisms of moisture transport in epoxy resins was performed by Christopher L. Soles et al. which developed a plausible molecular picture of the diffusion process [37]. In their analysis, the topology, polarity, and molecular motions combine to control transport. In

particular, the polarity of the resin is of relevant importance in determining the equilibrium concentration of water. They observed that less polar resins (non-amine series), absorb a little amount of water compared to the resins hardened with amines. It is worth noting that the intrinsic hole volume elements, active in the water transport, are localized at the crosslink junctions, which are also the locations of the polar hydroxyls and amines. The polar hydroxyls determine intersegmental and intrasegmental N---HO hydrogen bonds allowing water molecules to interact with the amine and hydroxyl groups. This type of interaction blocks the involved nanopores (hole volume elements) and impedes the water transport. In our case, even if the epoxy systems are solidified with the same hardener, a smaller number of nitrogen atoms, responsible of polar sites, are present in the resin solidified in non-stoichiometric conditions as highlighted by FT/IR analysis. Figure 15 shows the FTIR spectra of the samples solidified in non-stoichiometric condition containing embedded three types of nanofillers, in two different spectral ranges: a) 4000-500 $cm^{-1}$ and b) 1380-1170 $cm^{-1}$. The presence of nanofiller, at the investigated concentrations, seems to have small effect on the FT/IR spectra. In particular, for the sample filled with CpEG no differences with respect to other nanofillers are observed in the profile of the spectrum. This result highlights that the lower moisture content is due to factors almost independent of the chemical nature of the network in the epoxy matrix. As no large differences in the diffusion parameter are observed for the sample filled with CpEG with respect to other nanofillers, it is very likely that the lower moisture content is due to self-assembled effects which form structures entrapping part of the resin fraction and do not allow the interaction of water molecules with all the polar sites of the resin. This mechanism could also be active in parts of resin comprised between graphene sheets which partly enclose a fraction of the resin.

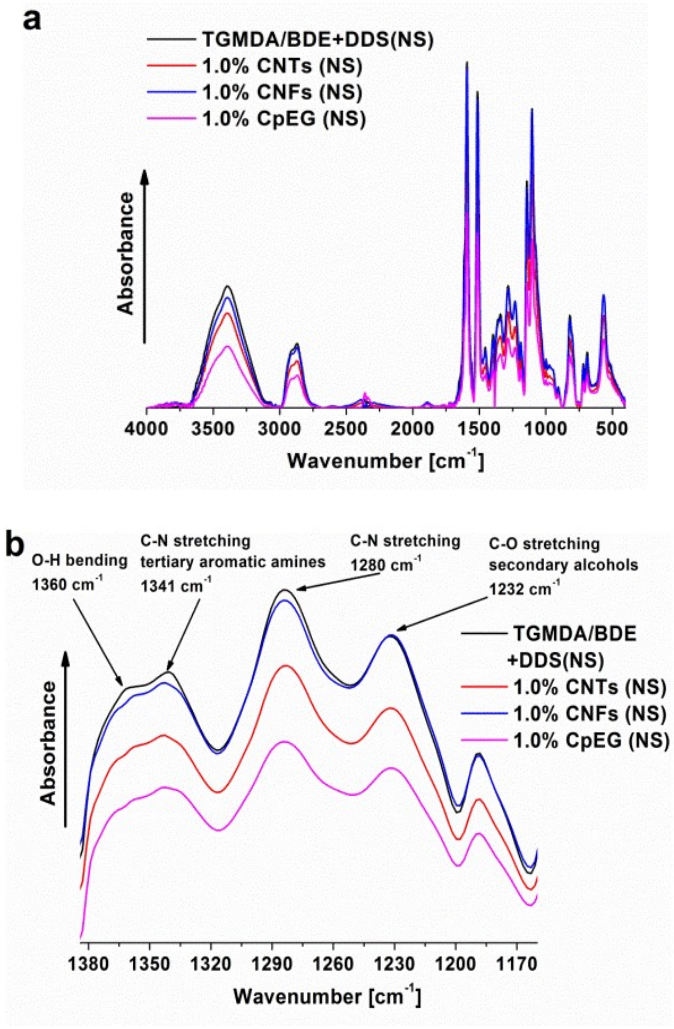


**Figure 15.** FTIR spectra of the samples solidified in non-stoichiometric condition containing embedded three types of nanofillers, in two different spectral ranges: a) 4000-500 $cm^{-1}$ and b) 1380-1170 $cm^{-1}$.

On the other hand, data in the previous section have shown that an impediment to the full cross-linking reactions caused by the nanofillers is observed. This impediment or interruption is localized in the zones surrounding the nanofillers. This effect is more marked for the sample loaded with CpEG with respect to CNTs and CNFs as highlighted by the entity of the peak at lower Tg which is more relevant for the resin loaded with CpEG (see dynamic mechanical results of Figure 11). This result also highlights that for the CpEG filler more extended zones of the surface areas strongly interact with the

epoxy matrix hindering not only the crosslinking reactions as previously discussed (see data on the Reaction enthalpies of Figure 10) but also the interaction of the polar sites of the resin with the water molecules.

### *3.5 Electrical Properties*

The electrical conductivity of nanocomposites exhibits a remarkable increase from that typical of the pure resin (few pS/m) to that of a conductor once the filler concentration increases over an electrical percolation threshold (EPT) due to the formation of conductive paths in the structure. Figure 16 shows the DC volume conductivity measured at room temperature as a function of the filler concentration (wt%) for the three types of carbon-based particles considered in the present study. Regardless of the filler and according to the percolation theory, as the filler amounts (i.e. $\phi$) increases beyond the threshold value ($\phi_c$), the electrical conductivity follows the classical power law (eq. 3):

$$\sigma = \sigma_0(\phi - \phi_c)^t \quad \text{(eq. 3)}$$

where $\sigma_0$ is the intrinsic conductivity of the filler and $t$ is a critical exponent depending on the dimensionality of the percolating structure. By increasing the filler percentage, higher values of electrical conductivity are achievied for all types of the resulting composites. More in detail, at the highest investigated concentration, i.e. 1 wt%, 2 wt% and 1,8 wt% for nanocomposites filled with CNTs, CNFs and CpEG, the corresponding conductivities reach the values of 0.29 S/m, 2 S/m and 0.096 S/m, respectively. Although the best performance in terms of electrical conductivity, for comparable reinforcement amounts are achieved by using filler of one-dimensional type (CNTs and CNFs), the potentially high aspect ratio of graphene sheets (i.e CpEG), defined for such type of filler as the ratio between its maximum lateral dimension and the thickness, combined with their phisical and chemical properties, may have favorable impact on improving the percolating network at low filler loadings. In fact, the experimental characterization reveals an interesting difference as it concerns

the electrical percolation threshold achieved with the three fillers. In particular, for both one-dimensional fillers (CNTs and CNFs), the EPT values fall in a comparable range, i.e. [0.1-0.32] and [0.05-0.32]%wt, respectively. Instead, the electrical percolation threshold is in a narrower interval [0.025-0.1]%wt for the composites reinforced with bi-dimensional CpEG filler. This means that CpEG reinforcements are able to create percolation conductive pathways more easily and with lower filler amounts through the insulating resin compared to the one-dimensional fillers. This result may be attributed to two mechanisms: the concentration of carboxylated groups localized at the edge of graphene sheets and the filler aspect ratio. The higher concentration of carboxylated groups responsible of attractive intermolecular bonding affects the filler/resin compatibility between the dispersed particles thus favoring the creation of the electrical networks with an "optimized" sort of self-assembled structures [19] (i.e. with shorter average distances betwen conductive fillers). Moreover, as it regards the filler aspect ratio (AR), different literature studies on carbon-based reinforced composites have identified this parameter as a critical factor [38-39]. In particular, the relationship $EPT \propto 1/AR$ can be adopted indicating that an higher aspect ratio leads to an improved electrical connectedness of the carbon-based network at lower filler amounts. Morphological analyses carried out on the fillers reveal an indicative AR of $[1, 1.6, 100]x10^3$ for CNT, CNF and CpEG respectively, thus confirming that an increase of the AR plays a key role in lowering the EPT in nanocomposites, in agreement with literature data [40]. From the insets of each percolation curve of Figure 16 reporting the log-log plots of the experimental conductivity vs. filler concentration, the characteristic parameters of the percolation law can be estimated. In particular, the value for the critical exponent *t* can be obtained as the slope of the linear fit.

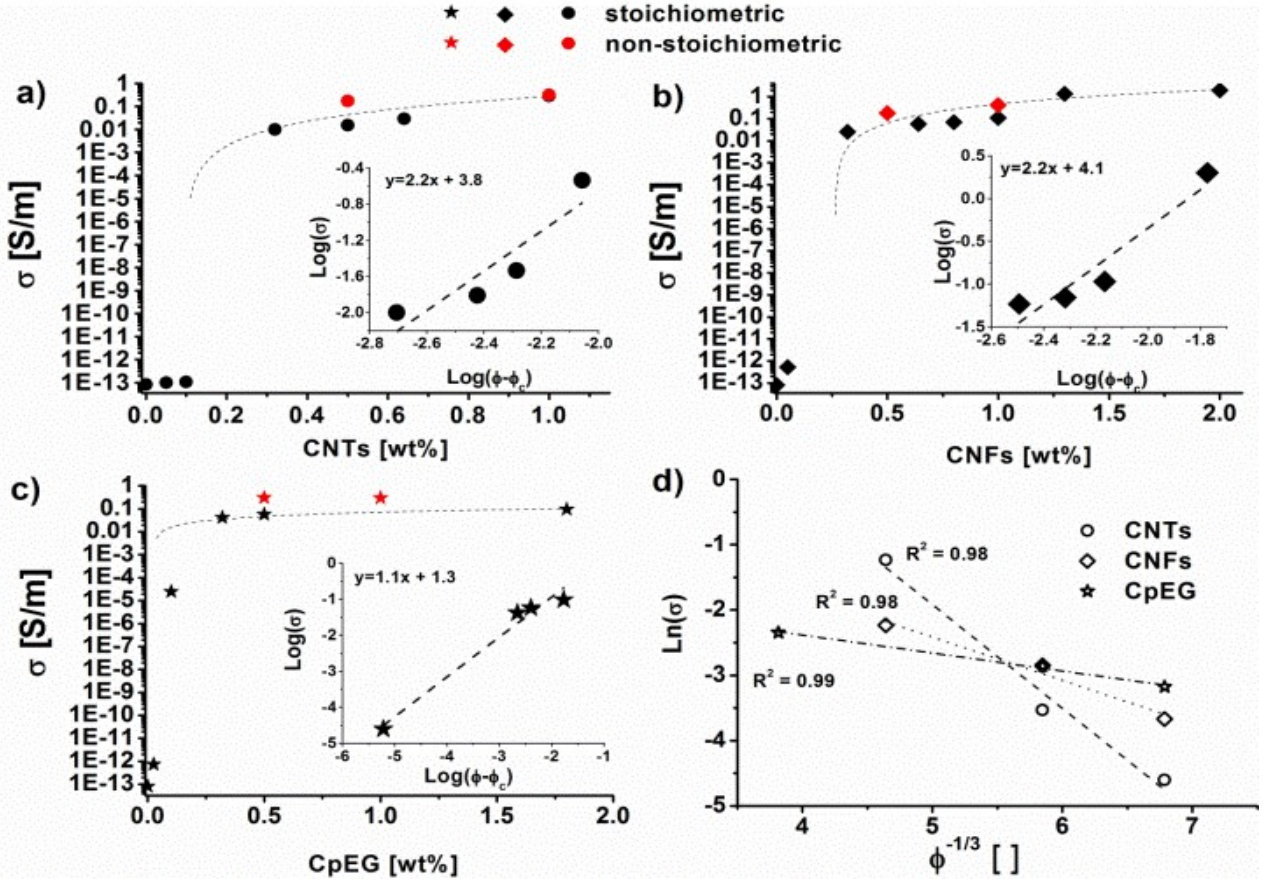


**Figure 16.** DC volume conductivity of the nanocomposites versus filler weight percentage. The inset shows the log-log plot of the electrical conductivity as a function of (ϕ-ϕc) with a linear fit for composites reinforced with a) CNTs; b) CNFs; c) CpEG. d) Plot of the natural logarithm of DC conductivity for sample above the EPT against ϕ-1/3. The dashed line is a fit of the DC data (marker) to eq. 5.

The estimated values, i.e. 2.2 for both CNTs and CNFs reinforced composites, are found to agree with universal values, reflecting an effective 3D organization of the percolating structure consistent with 1-D type of filler [41].

For composites filled with CpEG, it is interesting to note that the value of the exponent *t* decreases significantly showing a value equal to 1.1, since the nanoparticles exhibit two-dimensional shape. The presence of insulating resin around the carbon-based nanomaterials prevents direct electrical connection. This has been observed for example in amine-grafted MWCNT/epoxy composites in

which a thick polymer layer forms an extra phase on the carbon nanotube walls thus affecting the electrical properties of the resulting composite [5,9]. In the limit of a certain cut-off distance, the tunneling effect provides that electrons can flow through a barrier between adjacent electrically particles forming quantum tunneling junctions. The conduction mechanism in such a system can be modeled with a resistance $R_{tunnel}$ according to the following expression:

$$R_{tunnel} = \frac{h^2 d}{Ae^2\sqrt{2m\lambda}} exp^{\left(\frac{4\pi d}{h}\sqrt{2m\lambda}\right)} \qquad \text{(eq. 4)}$$

In the above equation $h$ is Planck's constant, $A$ and $d$ are the cross-sectional area and the distance between the filler (coincident with the thickness of the insulating resin wrapped around the particles) respectively, $e$ is the electron charge, $m$ is the mass of an electron and λ represents the height of the barrier which typically takes values of a few eV. It is evident as the tunneling effect depends strongly on the thickness of the insulating resin (i.e. $d$ ) around the filler that must be sufficiently thin to allow the tunneling conduction between neighbor conductive particles. Thicknesses larger than about 1.8 nm lead to composite conductivity values typical of an insulator material. A classic approach adopted in order to check if the electron tunneling is the main electrical transport mechanism in such nanofilled resins is to observe the occurence of the following relationship [6, 42-44]

$$\ln(\sigma) \propto \phi^{-1/3} \qquad \text{(eq. 5)}$$

i.e. a linear relation between the electrical conductivity (in logarithmic scale) and $\phi^{-1/3}$, valid for concentrations (ϕ) above the electrical percolation threshold. For our systems this is shown in Figure 16d. The dashed lines are fit curves of the experimental data (markers): the value of $R^2$ very close to 1 confirms the effectiveness of the tunneling modulated charge transport conjecture. As a consequence, the current and therefore the electrical conductivity of the resulting nanocomposites strongly depends on the interaction between the host matrix and the adopted filler and not only on the intrinsic conductivity of the latter [45]. In particular, the electrical properties are related to the morphology of

conductive network which in turn is affected by the dispersion technique and manufacturing process (i.e. cure temperature, chemical interactions between the filler and surrounding resin, etc.). Such results are also supported by the experimental characterization (see red markers in each percolation curve of Figure 16) carried out on nanocomposites prepared by stoichiometric and non-stoichiometric concentrations of hardener. For two selected filler concentrations of each carbon-based particle (i.e 0.5 wt% and 1 wt%), the electrical conductivity of the formulations with non-stoichiometric ratio of hardener are greater than the conductivity achieved in the stoichiometric case. This phenomenon is more evident for the 0.5 wt% concentration of filler since the conductivity increases of about one order of magnitude. In fact, in this case, the measured electrical conductivity varies from to 0.01 S/m up to 0.29 S/m and from 0.04 S/m up to 0.31 S/m for composites reinforced with CNTs and CpEG, respectively. The observed improvement in the electrical conductivity associated to the use of hardener in non-stoichiometric ratio could be ascribed to a reduction of the viscosity of the resin; in fact the decrease in viscosity promotes better dispersion of the particles within the hosting polymer thus favoring the creation of conductive electrical networks. Further study on this aspect entangling also the behavior of the dielectric properties of the nanocomposites is now underway and will be presented in a forthcoming paper.

### *3.6 General Consideration*

The CpEG sample is an interesting filler able to reduce moisture content and simultaneously enhance mechanical and electrical performance. This synergy between the different properties is hard to obtain and the choice of materials plays a crucial role. The performed work highlights that specific functionalizations can facilitate the attractive interaction at the interphase between the epoxy network and the nanofiller, enhancing in this way also the electrical percolation paths and the mechanical properties. In particular, the elemental composition (%wt) of CpEG sample indicates for C, H, and O

the values of 91.3, 0.2, 8.5 respectively and a value of ratio C/O of 10.7. The thermogravimetric curve of CpEG sample, under air atmosphere, shows two relevant mass loss stages at 300 and 659 °C, due to the removal of the groups containing oxygen and oxidation of carbon, respectively. The TGA curve evidences a content of about 10% of carboxylated groups (see Figure 17a).

On the other hand, the FT/IR spectrum of CpEG sample, together with the signal at 1740 $cm^{-1}$ due to the C=O stretching of ester groups, shows the intense peak at 1115 $cm^{-1}$ due to the signal of O-C-C stretching of aromatic esters, which falls between 1130 and 1100 $cm^{-1}$ because the conjugation modifies the wavenumbers with respect to aliphatic esters (see Figure 17b). This signal and therefore the presence of aromatic esters can be explained considering that in the phase of preparation of CpEG sample, some of the –OH of the carboxyl acids located on the edges of graphene layers condense with –OH groups. On the other hand, these groups, acting as hydrogen bonding moieties, are also responsible of intramolecular hydrogen bonding which contribute to the formation of nanofiller self-assembly structures through the matrix.

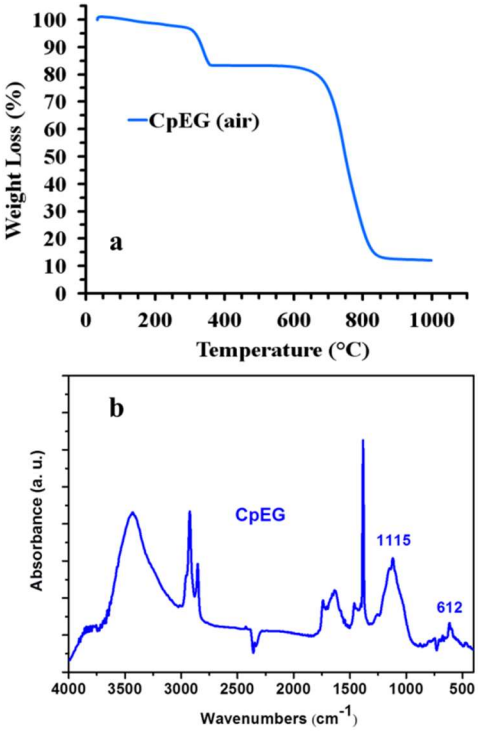


**Figure 17.** a) Thermogravimetric curve and b) FT/IR spectrum of CpEG powder.

It is very likely that the ease with which the electrical conductive paths form are due to the same mechanism. On the other hand, the carboxylic acid moieties are functional groups characterized by high value in the electric dipole moment. The strong polarity is due to the polarized carbonyl (C=O) and hydroxyl (O-H) groups. Is worth noting that the O-H group of carboxylic acids is even more polarized than the O-H group of alcohols due to the effect of adjacent carbonyl moiety in the molecular structure. An interesting consequence of these structural features is the enhancement in the dipole strength and hence the formation of energetically favorable hydrogen bonding (H-bonding) interactions also with the polar groups of the resin network. This specific last mechanism may favor electrical conductive paths and load transfers between matrix and nanofiller determining more marked mechanical reinforcements as shown in Figure 11e. For CpEG sample, the degree of exfoliation degree and role played by edge-carboxylated layers are key parameters in determining self-assembled

structures through the polymeric matrix as shown in the scheme of Figure 18. The red ellipses in Figure 18 highlight covalent bonds between edge carboxylated graphene layers, whereas the green one the role of the hydrogen-bond. They act as "attractive and cohesive forces" between the graphene particles dispersed inside the matrix and build blocks of complex systems outperforming the host matrix. This particular arrangement was considered responsible for the simultaneous improvements in electrical percolation threshold and mechanical performance. It is most likely that it is also one of the causes of the lower moisture content of the epoxy matrix filled with CpEG, together with the higher AR.

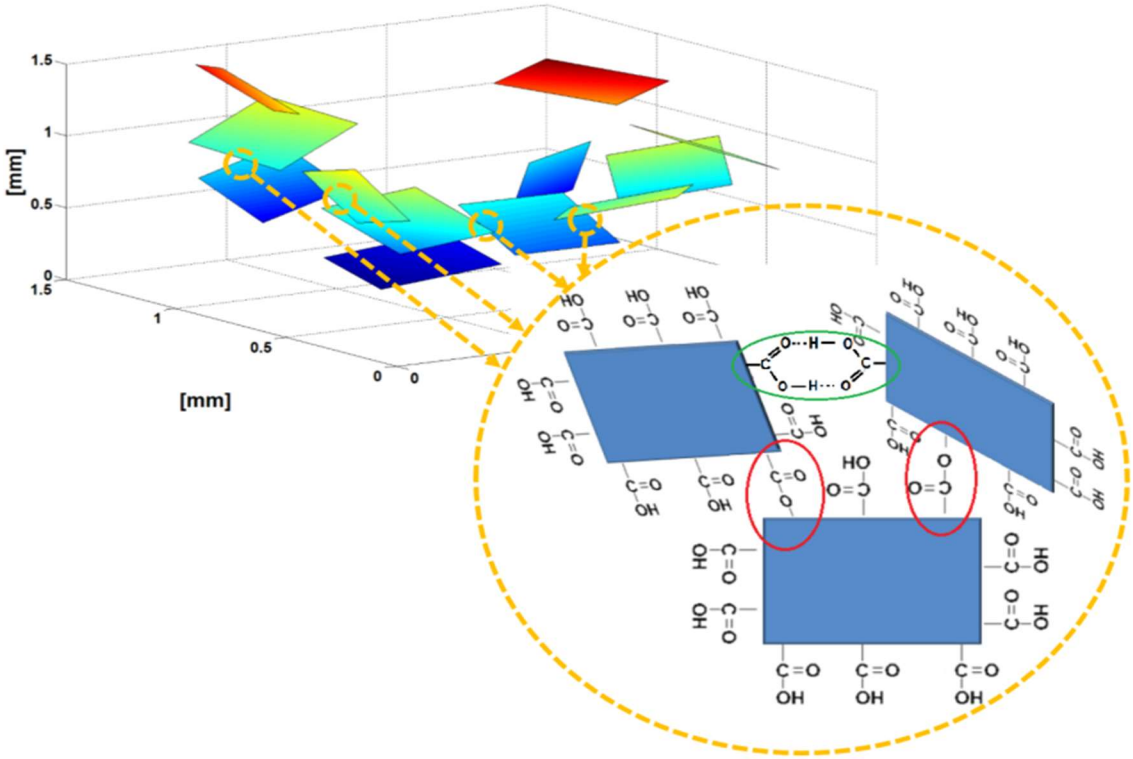


**Figure 18.** Schematic representation of the self-assembling of CpEG inside the matrix due to the presence of edge-carboxylated graphite layers. In the zoomed area here reported, the two considered bond-mechanisms are highlighted.

It is worth noting that among the graphene-based nanoparticles CpEG sample was chosen after a detailed study aimed at finding effective strategies to transfer some of excellent physical properties of

graphene layers to epoxy matrices. The evaluation of edge structures of very similar graphene-based materials, differing only for the amount of carboxylated group on the edges, highlighted that the effect on the electrical, mechanical and transport properties is impressive. The chemistry of graphene edges can be responsible of significant improvements in the physical properties of the nanofilled resin. In fact, resins loaded with CpEG constituted by 40% of graphite with a correlation length perpendicular to the structural layers of 9.8 nm (crystalline lengths perpendicular to reflection planes 002) and 60% of exfoliated graphene, with an amount of carboxylated groups of about 10% on the edges, are characterized by electrical percolation threshold that can be achieved with nanofiller concentration less than 0.5% by weight. This value of nanofiller concentration allows to reach DC electrical conductivity raging between 0.1-1 S/m. As for the good performance in transport properties, the good electrical and mechanical performance can be ascribed to self-assembly mechanisms determined by attractive interactions between edge-carboxylated graphene particles. It is worth noting that the composition of the graphene-based nanoparticles (CpEG) gives particular advantages to combine the described properties. In fact, it was highlighted that, for bulk samples, single graphene layers (without defects) tend to reassemble during the manufacturing process of the nanofilled samples. On the other hand, the reassembling of graphene layers can be avoid functionalizing the graphene layers. In fact, functional groups attached to the graphene layers prevent the re-assembling of layers because of steric and energy factors. However, in this occurrence, due to the transition from $sp^2$ to $sp^3$-hybridization of carbon atoms, functionalized single layers (SL) of graphene tend to lose part of the delocalized electrons and, therefore, the electronic properties of graphene with a consequent reduction in the electrical conductivity of the nanocomposites. Furthermore, the changes in the hybridization state of the carbon atoms also cause a strong deviation from the planarity structure of the graphene layers. This structural and morphological feature further worsen the difficulty of single layers to form conductive paths inside the bulk polymeric matrix. Therefore, significant benefits in the multifunctionality performance (simultaneous improvements in the mechanical, electrical, water

transport properties) can be achieved embedding in the polymeric matrix ultrathin graphitic layers which preserving a large number of $sp^2$-hydridized carbon atoms, also preserve the graphene-like electronic properties. A tailored control in chemistry and morphological parameters of graphene-based nanoparticles may be responsible of drive relevant changes at nanoscale level which are able to enhance in a synergic way the beneficial effects of graphene-based nanoparticles for bulk samples.

## 4. Conclusion

Multifunctional epoxy mixtures able to decrease the moisture content and increase electrical and mechanical properties have been designed and realized. The sorption at equilibrium of liquid water ($C_{eq}$) decreases from 6.81% to 5.76% for the sample TGMDA/BDE+DDS solidified in stoichiometric concentration of hardener and to 4.83% for the sample TGMDA/BDE+80DDS(NS) solidified in non-stoichiometric condition. The resin reduces the value in $C_{eq}$ from a minimum of 15% at a maximum of 30%. This percentage is very relevant for many industrial applications. Samples loaded with CNTs, CNFs and CpEG are characterized by values of Ceq only slightly higher than the unfilled matrix. The composites obtained with CpEG are characterized by the lowest value, among all considered systems, of the moisture content. It has also been found that the nanocomposite filled with CpEG is characterized by low electrical percolation threshold (EPT) that falls in the narrow interval [0.025-0.1]%wt and improved mechanical properties. The self-assembly of layers due to the attractive interactions between edge-carboxylated graphene particles was found to favor the electrical percolative paths. Edge-carboxylation also increases the nanofiller/epoxy matrix interaction determining a relevant reinforcement in the elastic modulus. The controllable feature of the nanoparticles can be an alternative parameter to design epoxy resins where high electrical conductivity is required at very low filler concentration. Data here shown highlight that nanocomposites obtained using the epoxy matrix hardened in non-stoichiometric condition are also able to further enhance the

electrical conductivity; at 0.5% of filler, an increase in the electrical conductivity of 1 order of magnitude is observed. In fact, the measured electrical conductivity varies from to 0.01 S/m up to 0.29 S/m and from 0.04 S/m up to 0.31 S/m for composites reinforced with CNTs and CpEG, respectively. Hence, CpEG nanoparticles at 0.5% by weight, are particularly able to increase electrical conductivity and reduce the moisture content making them particularly advantageous for applications in the field of the wind energy, aviation and shipbuilding.

Self-assembling effects can be also responsible for the lower moisture content. Self-assembled structures can entrap part of the resin fraction hindering the interaction of water molecules with all the polar sites of the resin. This mechanism could also be active in parts of resin in contact with graphene/graphitic layers or comprised between graphene sheets which partially enclose a fraction of the resin. Dynamic mechanical results have shown that all the analyzed fillers tend to create a phase with increased mobility of the chains, segmental parts of the epoxy network around the filler which causes an increase in the more mobile phase. This effect is more marked for the sample loaded with CpEG highlighting that more extended zones are in contact with the nanofiller. This particular structural/morphological arrangement due to the nature of the functionalization and the nanofiller CpEG is most likely responsible to better hinder the interaction of the polar sites of the resin with the water molecules as highlighted before.

Furthermore, in this manuscript, many aspects related to the variation of the Tg due to the inclusion of the nanofiller in the resin have been analyzed. Concerning this aspect, it is worth noting that, so far the influence of carbon nanotubes on both the cure kinetics and the physical properties of the resins has been reported, in particular considering the variation of the glass transition temperature for pristine resin and in presence of CNTs. However, conflicting results have been reported and the effect of CNTs on the Tg needed to be clarified. In this paper, we have analyzed the unfilled resin hardened in stoichiometric and non-stoichiometric condition to better understand the effect of different nanofillers on the Tg of the nanocomposites. Results here discussed highlight that the impossibility to extend the

tri-dimensional network in the space filled by the nanoparticles is responsible of a more mobile phase determining an additional Tg at lower temperature with respect to the main glass transition temperature.

Concerning the effect of nanofiller on the resin hardened in non-stoichiometric conditions, a synergism between nanofiller effect and low DDS level is observed. The fraction of the more mobile phase and the temperature range where the movements of the molecular segments are activated are strictly related to the amount and nature of the nanofiller.

## Acknowledgements

The research leading to these results has received funding from the European Union's Seventh Framework Programme for research, technological development and demonstration under Grant Agreement N° 313978. The author thank Prof. Gaetano Guerra from the Department of Chemistry and Biology, University of Salerno for very useful discussions.

## References

[1] Scelsi L, Bonner M, Hodzic A, Soutis C, Wilson C, Scaife R and Ridgway K 2011 *eXPRESS Polym. Lett.* **5** 209-17

[2] Domun N, Hadavinia H, Zhang T, Sainsbury T, Liaghata G H and Vahida S 2015 *Nanoscale* **7** 10294-329

[3] Larsson A 2002 *C. R. Phys.* **3** 1423-1444

[4] Petrov N, Haddad A, Griffiths H and Waters R, In Lightning Strikes to Aircraft Radome: Electric Field Shielding Simulation, 17th International Conference on Gas Discharges and Their Applications, Cardiff - UK, 7-12 september, 2008

[5] Guadagno L, De Vivo B, Di Bartolomeo A, Lamberti P, Sorrentino A, Tucci V, Vertuccio L and Vittoria V 2011 *Carbon* **49** 1919-30

[6] Guadagno L, Raimondo M, Vittoria V, Vertuccio L, Naddeo C, Russo S, De Vivo B, Lamberti P, Spinelli G and Tucci V 2014 *RSC Adv.* **4** 15474-88

[7] Zhou Y, Wu P, Cheng Z, Ingram J and Jeelani S 2008 *eXPRESS Polym. Lett.* **2** 40-8

[8] Yasmin A and Daniel I M 2004 *Polymer* **45** 8211-9

[9] Kotsilkova R, Ivanov E, Bychanok D, Paddubskaya A, Demidenko M, Macutkevic J, Maksimenko S and Kuzhir P 2015 *Compos. Sci. Technol.* **106** 85-92

[10] Maxwell I D and Pethrick R A 1983 *J. Appl. Polym. Sci.* **28** 2363-79

[11] Liu W, Hoa S V and Pugh M 2005 *Compos. Sci. Technol.* **65** 2364-73

[12] Li L, Yu Y, Wu Q, Zhan G and Li S 2009 *Corros. Sci.* **51** 3000-6

[13] Sarti G C and Apicella A 1980 *Polymer* **21** 1031-6

[14] Thomas N and Windle A A 1980 *Polymer* **21** 613-9

[15] Guadagno L, Raimondo M, Vittoria V, Vertuccio L, Naddeo C, Lamberti P, Tucci V and Russo S, Epoxy Resin with Low Humidity Content. *European Patent Application* EP2873682 (A1), 2015. Also published as: ITTO20130926 (A1) - Resina epossidica con basso tenore di umidità.

[16] Nobile M R, Raimondo M, Lafdi K, Fierro A, Rosolia S and Guadagno L 2015 *Polym. Compos.* **36** 1152-60

[17] Guadagno L, Raimondo M, Vietri U, Vertuccio L, Barra G, De Vivo B, Lamberti P, Spinelli G, Tucci V and Volponi R 2015 *RSC Adv.* **5** 6033-42

[18] Guadagno L, Raimondo M, Vittoria V, Vertuccio L, Lafdi K, De Vivo B, Lamberti P, Spinelli G and Tucci V 2013 *Nanotechnology* **24** 305704

[19] Guadagno L, Raimondo M, Vertuccio L, Mauro M, Guerra G, Lafdi K, De Vivo B, Lamberti P, Spinelli G and Tucci V 2015 *RSC Adv.* **5** 36969-78

[20] Geim A K and Novoselov K S 2007 *Nat. Mater.* **6** 183-191

[21] Eda G, Fanchini G and Chhowalla M 2008 *Nat. Nanotechnol.* **3** 270-4

[22] Kim K S, Zhao Y, Jang H, Lee S Y, Kim J M, Kim K S, Ahn J H, Kim P, Choi J Y, Hong B H 2009 *Nature* **457** 706-10

[23] Blake P, Brimicombe P D, Nair R R, Booth T J, Jiang D, Schedin F, Ponomarenko L A, Morozov S V, Gleeson H F and Hill E W 2008 *Nano Lett.* **8** 1704-8

[24] Vietri U, Guadagno L, Raimondo M, Vertuccio L and Lafdi K 2014 *Compos Part B - Eng* **61** 73-83

[25] Dikin D A, Stankovich S, Zimney E J, Piner R D, Dommett G H, Evmenenko G, Nguyen S T and Ruoff R S 2007 *Nature* **448** 457-60

[26] Bunch J S, Verbridge S S, Alden J S, Van Der Zande A M, Parpia J M, Craighead H G and McEuen P L 2008 *Nano Lett.* **8** 2458-62

[27] Yan N, Buonocore G, Lavorgna M, Kaciulis S, Balijepalli S K, Zhan Y, Xia H and Ambrosio L 2014 *Compos. Sci. Technol.* **102** 74-81

[28] Scherillo G, Lavorgna M, Buonocore G G, Zhan Y H, Xia H S, Mensitieri G and Ambrosio L 2014 *ACS Appl. Mater. Interfaces* **6** 2230-4

[29] Guadagno L, Sarno M, Vietri U, Raimondo M, Cirillo C and Ciambelli P 2015 *RSC Adv.* **5** 27874-86

[30] Guadagno L, Vertuccio L, Sorrentino A, Raimondo M, Naddeo C, Vittoria V, Iannuzzo G, Calvi E and Russo S 2009 *Carbon* **47** 2419-30

[31] Vertuccio L, Russo S, Raimondo M, Lafdi K and Guadagno L 2015 *RSC Adv.* **5** 90437-50

[32] May C and Weir F 1962 *Polym. Eng. Sci.* **2** 207-12

[33] Pogany G 1970 *Polymer* **11** 66-78

[34] Zhou T, Wang X, Liu X and Xiong D 2009 *Carbon* **47** 1112-8

[35] Allaoui A, Bai S, Cheng H M and Bai J 2002 *Compos. Sci. Technol.* **62** 1993-8

[36] Allaoui A and El Bounia N E 2009 *eXPRESS Polym. Lett.* **3** 588-94

[37] Soles C L and Yee A F 2000 *J. Polym. Sci., Part B: Polym. Phys.* **38** 792-802

[38] Shehzad K, Dang Z M, Ahmad M N, Sagar R U R, Butt S, Farooq M U and Wang T B 2013 *Carbon* **54** 105-12

[39] De Vivo B, Lamberti P, Spinelli G, Tucci V, Guadagno L and Raimondo M 2015 *J. Appl. Phys.***118** 064302

[40] Bellucci S, Bistarelli S, Cataldo A, Micciulla F, Kranauskaite I, Macutkevic J, Banys J, Volynets N, Paddubskaya A and Bychanok D 2015 *IEEE Trans. Microw. Theory Techn.* **63** 2024-31

[41] Nan C W, Shen Y and Ma J 2010 *Annu. Rev. Mater. Res.* **40** 131-51

[42] Connor M T, Roy S, Ezquerra T A and Calleja F J B 1998 *Phys. Rev. B* **57** 2286

[43] Mdarhri A, Carmona F, Brosseau C and Delhaes P 2008 *J. Appl. Phys.* **103** 054303

[44] Kilbride B E, Coleman J, Fraysse J, Fournet P, Cadek M, Drury A, Hutzler S, Roth S and Blau W 2002 *J. Appl. Phys.* **92** 4024-30

[45] Plyushch A, Macutkevic J, Kuzhir P, Banys J, Bychanok D, Lambin P, Bistarelli S, Cataldo A, Micciulla F and Bellucci S 2016 *Compos. Sci. Technol.* **128** 75-83